DEVELOPMENT OF QUALITY STANDARDS FOR INCLUSION OF HIGH RECYCLED ASPHALT PAVEMENT CONTENT IN ASPHALT MIXTURES – PHASE II

TR-658

Final Report
March 2015

Sponsored by
Iowa Highway Research Board

Hosin "David" Lee, Principal Investigator
Clint Van Winkle, Graduate Research Assistant
Ali Mokhtari, Graduate Research Assistant
Taha Ahmed, Postdoctoral Research Scholar
Haena Kim, Graduate Research Assistant

Public Policy Center
University of Iowa

Chris Williams, Co-Principal Investigator
Sheng Tang, Graduate Research Assistant

InTrans
Iowa State University

Disclaimer

The contents of this report reflect the views of the authors, who are responsible for the facts and the accuracy of the information presented herein. The opinions, findings, and conclusions expressed in this publication are those of the authors and not necessarily those of the sponsors.

The sponsors assume no liability for the contents or use of the information contained in this document. This report does not constitute a standard, specification, or regulation. The sponsors do not endorse products or manufacturers. Trademarks or manufacturers' names appear in this report only because they are considered essential to the objectives of the document.

Statement of Non-Discrimination

Federal and state laws prohibit employment and/or public accommodation discrimination on the basis of age, color, creed, disability, gender identity, national origin, pregnancy, race, religion, sex, sexual orientation or veteran's status. If you believe you have been discriminated against, please contact the Iowa Civil Rights Commission at 800-457-4416 or Iowa Department of Transportation's affirmative action officer. If you need accommodations because of a disability to access the Iowa Department of Transportation's services, contact the agency's affirmative action officer at 800-262-0003.

1. REPORT NO.	2. GOVERNMENT ACCESSION NO.	3. RECIPIENT'S CATALOG NO.
TR-658		

4. TITLE AND SUBTITLE
DEVELOPMENT OF QUALITY STANDARDS FOR INCLUSION OF HIGH RECYCLED ASPHALT PAVEMENT CONTENT IN ASPHALT MIXTURES – PHASE II

5. REPORT DATE
March 2015

6. PERFORMING ORGANIZATION CODE

7. AUTHOR(S)
Hosin “David” Lee, Clint Van Winkle, Russell Carlson, Ali Mokhtari, Taha Ahmed, Haena Kim, Sheng Tang, Chris Williams

8. PERFORMING ORGANIZATION REPORT NO.

9. PERFORMING ORGANIZATION NAME AND ADDRESS
Public Policy Center
University of Iowa
227 South Quadrangle
Iowa City, IA 52242-1192

10. WORK UNIT NO.

11. CONTRACT OR GRANT NO

12. SPONSORING AGENCY NAME AND ADDRESS
Iowa Highway Research Board
Iowa Department of Transportation
800 Lincoln Way, Ames, IA 50010

13. TYPE OF REPORT AND PERIOD COVERED
Final Report

14. SPONSORING AGENCY CODE

15. SUPPLEMENTARY NOTES

16. ABSTRACT
To conserve natural resources and energy, the amount of recycled asphalt pavement has been steadily increasing in the construction of asphalt pavements. The objective of this study is to develop quality standards for inclusion of high RAP content. To determine if the higher percentage of RAP materials can be used on Iowa’s state highways, three test sections with target amounts of RAP materials of 30%, 35% and 40% by weight were constructed on Highway 6 in Iowa City. To meet Superpave mix design requirements for mixtures with high RAP contents, it was necessary to fractionate the RAP materials. Three test sections with actual RAP materials of 30.0%, 35.5% and 39.2% by weight were constructed and the average field densities from the cores were measured as 95.3%, 94.0%, and 94.3%, respectively. Field mixtures were compacted in the laboratory to evaluate moisture sensitivity using a Hamburg Wheel Tracking Device. After 20,000 passes, rut depths were less than 3mm for mixtures obtained from three test sections. The binder was extracted from the field mixtures from each test section and tested to identify the effects of RAP materials on the performance grade of the virgin binder. Based on Dynamic Shear Rheometer and Bending Beam Rheometer tests, the virgin binders (PG 64-28) from test sections with 30.0%, 35.5% and 39.2% RAP materials were stiffened to PG 76-22, PG 76-16, and PG 82-16, respectively. The Semi-Circular Bending (SCB) test was performed on laboratory compacted field mixtures with RAP amounts of 30.0%, 35.5% and 39.2% at two different temperatures of -18 and -30 °C. As the test temperature decreased, the fracture energy decreased and the stiffness increased. As the RAP amount increased, the stiffness increased and the fracture energy decreased. Finally, a condition survey of the test sections was conducted to evaluate their short-term pavement performance and the reflective transverse cracking did not increase as RAP amount was increased from 30.0% to 39.2%.

17. KEY WORDS
recycled asphalt pavement, high RAP content, fractionation methods, high RAP mix design, Semi-Circular Bending test

18. DISTRIBUTION STATEMENT
No restrictions.

19. SECURITY CLASSIF. (of this report)	20. SECURITY CLASSIF. (of this page)	21. NO. OF PAGES	22. PRICE
None	None	47	N/A

Technical Advisory Committee

Scott Schram, Iowa DOT, Scott.Schram@dot.iowa.gov

Jeffrey Schmitt, Iowa DOT, Jeffrey.schmitt@dot.iowa.gov

Bill Rosener, APAI, billr@apai.net

Larry Mattusch, APAI, lmatt2@mchsi.com

Guy Sisler, Flint Hills Resources, guy.sisler@fhr.com

Marla Kilburg, Flint Hills Resources, marla.kilburg@fhr.com

John Hinrichsen, Hinrichsen.john@yahoo.com

Gary Netser, L.L. Pelling, garyn@llpelling.com

Chuck Finnegan, L.L. Pelling, chuckf@llpelling.com

TABLE OF CONTENTS

LIST OF TABLES

LIST OF FIGURES

ABSTRACT

To conserve natural resources and energy, the amount of recycled asphalt pavement has been steadily increasing in the construction of asphalt pavements. The objective of this study is to develop quality standards for inclusion of high RAP content. To determine if the higher percentage of RAP materials can be used on Iowa's state highways, three test sections with target amounts of RAP materials of 30%, 35% and 40% by weight were constructed on Highway 6 in Iowa City. To meet Superpave mix design requirements for mixtures with high RAP contents, it was necessary to fractionate the RAP materials. Three test sections with actual RAP materials of 30.0%, 35.5% and 39.2% by weight were constructed and the average field densities from the cores were measured as 95.3%, 94.0%, and 94.3%, respectively. Field mixtures were compacted in the laboratory to evaluate moisture sensitivity using a Hamburg Wheel Tracking Device. After 20,000 passes, rut depths were less than 3mm for mixtures obtained from three test sections. The binder was extracted from the field mixtures from each test section and tested to identify the effects of RAP materials on the performance grade of the virgin binder. Based on Dynamic Shear Rheometer and Bending Beam Rheometer tests, the virgin binders (PG 64-28) from test sections with 30.0%, 35.5% and 39.2% RAP materials were stiffened to PG 76-22, PG 76-16, and PG 82-16, respectively. The Semi-Circular Bending (SCB) test was performed on laboratory compacted field mixtures with RAP amounts of 30.0%, 35.5% and 39.2% at two different temperatures of -18 and -30 °C. As the test temperature decreased, the fracture energy decreased and the stiffness increased. As the RAP amount increased, the stiffness increased and the fracture energy decreased. Finally, a condition survey of the test sections was conducted to evaluate their short-term pavement performance and the reflective transverse cracking did not increase as RAP amount was increased from 30.0% to 39.2%.

1 INTRODUCTION

Recycled asphalt pavement (RAP) has been used for many years in the United States and it is considered as the world's most recycled product. In Iowa, the proportion of asphalt binder from RAP can be allowed up to 20% of the total binder content without changing the prescribed standard virgin asphalt grade. When more than 20% RAP by binder replacement is used, testing of the RAP's recovered binder is recommended to determine a proper performance grade of virgin binder to be used (McDaniel et al. 2000). However, there was no significant difference in laboratory performance test results between the high RAP mixes (between 21% and 30%) and the low RAP mixes (20% or less) (Maupin et al. 2008). It was reported that viable mixes with higher RAP contents of up to 50% by binder replacement could be designed (McDaniel et al. 2002). In 2008, the NAPA set a goal to double the national average RAP content from 12 percent to 24 percent in the next five years (NCAT 2010).

There is a lack of understanding about how the binder from the RAP contributes to the overall mix. Viewpoints range from the RAP binder completely blends with the virgin binder to that it does not blend at all (i.e., RAP acts in the mix like a "black rock"). The Illinois DOT assumes 100% contribution for the residual asphalt binder from the RAP which reduces the requirement for virgin asphalt binder by the full amount of asphalt binder in the RAP. However, this assumption has been reported to be inaccurate and thus could result in an erroneous Hot Mix Asphalt (HMA) job mix formula causing dry HMA (Al-Qadi et al. 2007). Several studies have shown the contribution of RAP binder is somewhere in between these two theories by examining the rheology of the resulting binder (Stephens et al. 2001; Huang et al. 2005; Bennert et al. 2014).

Most agencies limit the quantity of RAP materials in asphalt mixtures and/or the amount of recycled binder. For example, the Iowa DOT limits the use of RAP materials up to 15% by weight for the surface course while at least 70% of the total asphalt binder shall be virgin asphalt. A contractor is allowed to use more than 15% when there is quality control sampling and testing of the RAP materials meeting the requirements in the specification (Iowa-DOT 2010). It has been reported that mixes with up to 40% RAP materials by weight have performed better than mixes with 20% RAP materials in Hamburg Wheel Tracking test (Boriack 2014; Diefenderfer and Nair 2014).

Without fractionating RAP materials, however, it is difficult to meet the mix design criteria. Agencies have been successful in utilizing as much as 50% Fractionated RAP (FRAP) materials, which would remove fine RAP materials passing a specific sieve size. Because FRAP materials include less fine materials, it is feasible to produce mixtures that would meet Superpave mix design requirements. For example, the Wisconsin DOT requires that at least 80% of the total asphalt binder should be virgin but it may be reduced to 75% when FRAP is used. Contractors may further reduce a percentage of virgin binder below 75% if they can provide test results indicating the resultant binder meets the originally specified grade (Wisconsin DOT 2009). In Florida, State Road 15A was successfully constructed using asphalt mixtures containing 45 percent FRAP (Udelhofen 2007). In Overland Park in Kansas, where the DOT limits the use of RAP to 20-25% without binder modification, the Antioch road under a high volume of traffic was constructed using 35% FRAP mix meeting the Superpave mix design (Udelhofen 2010).

The main objective of this project is to develop quality standards for inclusion of high RAP content in asphalt mixtures. A primary concern with high-RAP content mixtures is the resultant performance grade of the blended asphalt binder. Many state DOT specifications require the use of a 'softer' virgin asphalt binder (i.e. lower PG grade) when the RAP materials account for a certain percentage of virgin binder replacement or mixture weight.

This report presents both laboratory and field evaluation results of three test sections with target amounts of RAP materials of 30%, 35%, and 40% by weight. However, due to limitations in dispensing RAP materials in the field, the actual amounts of RAP materials used to build the test sections were 30.0%, 35.5% and 39.2% by weight. First, a sieve-by-sieve analysis was performed on the RAP material to identify the optimum sieve size to fractionate RAP materials. Field mixtures were then tested for their moisture sensitivity using a Hamburg Wheel Tracking (HWT) device and the low-temperature cracking using Semi-Circular Bending (SCB) test. To identify the effect of RAP on the virgin binder, the binder was extracted from the field mixtures to determine the performance grade. Finally, to compare the short-term performance of three test sections with varying amounts of RAP, a condition survey has been performed.

The results of the research is presented as new asphalt mix design with high RAP contents, which was used to design asphalt mixtures with varying RAP contents for the test sections. Both asphalt binder and mixture tests have been performed at all temperature regimes to characterize the binder contained in RAP materials. In addition, this study explored the possible role that fractionation may take in increasing RAP usage. Test sections with varying RAP contents were monitored for their relative amounts of reflective cracking in the field. Laboratory tests and field performance of asphalt mixtures with high RAP contents would help pavement engineers design asphalt mixtures with optimum RAP contents and increase the use of RAP materials while enhancing the long-term performance of pavements in Iowa.

2 RECYCLED ASPHALT PAVEMENT MATERIALS

As shown in Table 2-1, Iowa DOT has adopted the categorization system that classifies the RAP stockpiles into three types: classified RAP, certified RAP and unclassified RAP so that the RAP materials with high-quality aggregate properties are allowed to be used in various amounts in different pavement layers. The maximum RAP percentage allowed in surface course mixtures is limited due to the exposure to traffic loading and environmental conditions. The maximum allowable RAP usage for the surface layer is further reduced for higher ESAL pavements. The Iowa DOT specifications are on the conservative side of the Midwestern region by only allowing a maximum of 15% Classified RAP usage in the surface course for any ESAL category and only 10% Certified RAP in the surface course for pavements with less than or equal to 300,000 ESAL's.

Table 2-1: Iowa DOT RAP Stockpile Categorization Criteria & Allowable Usage

	Classified RAP	Certified RAP	Unclassified RAP
Requirements	Documented source High Aggregate Quality Stockpiled Separately Meets Quality Control	Undocumented Source Lower Aggregate Quality Poor Stockpiling Meets Quality Control	Undocumented source Unknown/Poor Aggregate Poor Stockpiling No Quality Control
Allowable Usage	15% weight in surface Min. 70% virgin AC No limit in other layers	10% surface $\leq$ 300K ESAL 20% Interm. $\leq$ 1M ESAL 20% Base for all ESAL	0% surface for all ESAL 10% Interm. $\leq$ 1M ESAL 10% Base for all ESAL

Source: Section 2303. Hot Mix Asphalt Mixtures. Iowa DOT Standard Specifications

2.1 Fractionated RAP Materials from I-80

Samples of RAP materials were obtained from classified RAP stockpiles at L.L. Pelling Company's asphalt plant. Millings were obtained at a high speed and a shallow depth from the surface, resulting in a small amount of dust content of 10.7%. The purpose of these RAP fractionation methods was to create new stockpiles with reduced fine aggregate composition. As shown in Table 2-2, a component analysis was performed on the RAP stockpile from I-80. An excessive amount of RAP materials passing No. 200 sieve is the main cause for not meeting the gradation requirements. Based on the sieve-by-sieve analysis of RAP materials, RAP materials passing 5/16" sieve were discarded. The gradation of RAP materials retained on a 5/16" sieve was very consistent and the dust content was low whereas the fine RAP materials passing 5/16" sieve exhibited higher recovered asphalt binder content and high dust content.

Table 2-2: Sieve-Size-Separated RAP Material Composition Analysis

Size of RAP	Recovered Aggregate Composition After Ignition Oven Burn-Off – (% Retained)											Asphalt Content %	% of Stockpile	% of Dust Content
	¾”	½”	3/8”	No. 4	No. 8	No. 16	No. 30	No. 50	No. 100	No. 200	Pan			
1 1/2”	0.0	3.9	4.7	27.5	20.1	13.9	9.6	7.6	3.8	1.4	7.6	**4.66**	**4.15**	**3.30**
1”	0.0	5.5	5.7	27.7	18.8	12.8	8.7	7.6	3.8	1.4	8.0	**4.78**	**5.54**	**4.61**
¾”	1.1	1.1	10.0	6.2	27.6	16.2	10.9	8.3	7.8	3.7	7.2	**4.61**	**6.41**	**4.79**
½”	---	20.8	10.6	20.8	13.6	9.6	7.0	6.2	3.3	1.2	7.0	**4.09**	**12.68**	**9.26**
3/8”	---	---	39.81	21.9	10.2	7.2	5.2	5.0	2.7	1.0	5.7	**3.62**	**8.62**	**5.11**
No. 4	---	---	---	56.1	15.8	7.2	5.4	5.3	2.8	1.0	5.4	**3.66**	**22.18**	**14.91**
No. 8	---	---	---	---	65.2	12.0	5.5	5.7	3.1	1.1	7.5	**4.43**	**15.56**	**12.13**
No. 16	---	---	---	---	---	61.7	13.6	7.4	3.9	1.6	11.8	**5.55**	**10.38**	**12.82**
No. 30	---	---	---	---	---	---	60.8	14.9	5.0	1.9	17.4	**6.72**	**6.12**	**11.13**
No. 50	---	---	---	---	---	---	---	67.2	7.4	2.5	23.0	**7.98**	**4.35**	**10.45**
No. 100	---	---	---	---	---	---	---	---	64.2	7.5	28.3	**9.34**	**2.08**	**6.15**
No. 200	---	---	---	---	---	---	---	---	---	57.2	42.8	**9.74**	**0.98**	**4.37**
Normalized Composite	0	3	6	20	20	14	10	9	5	2.1	9.6	**4.75**	**99.1%**	**99.1%**
Binder Extraction	0	2	5	21	20	14	11	10	4	2.3	10.7	**4.00**		
Estimated Coarse RAP	0	5	10	34	16	10	7	6	4	1.4	6.7	**4.02**	**59.6%**	**42.0%**
Estimated Fine RAP	0	0	0	0	26	21	15	14	7	3.2	13.8	**5.86**	**40.4%**	**58.0%**

3 INFLUENCE OF RAP ON BINDER GRADE

3.1 Test Sections

Figure 3-1 shows the layout of the test sections located on the westbound inside lane of Highway 6 in Iowa City. The existing concrete pavement was observed to be severely damaged throughout the test sections. Test sections were constructed by LL Pelling Company with HMA mixtures produced from the plant in Coralville, Iowa. The 1.5-inch thick surface layer was constructed on top of 1.5-inch thick intermediate layer. The 1.5-inch thick surface layers in the three test sections were started to be placed at 7:00 pm on September 8, 2013 and completed at 5:00 a.m. next day. Three test sections with actual RAP contents of 30.0%, 35.5% and 39.2% were constructed. The 30.0% RAP test section starts at Lakeshore Dr. and ends at Fairmeadows Boulevard with a total length of about 0.5 miles. The 35.5% RAP starts at Fairmeadows Boulevard and continues for another 0.5 miles to the Sycamore Street intersection. The 39.2% RAP section is also 0.5 mile long and starts at the Sycamore Street intersection and ends at the Broadway St. intersection. The traffic level for the project is approximately 13,100 ADT.

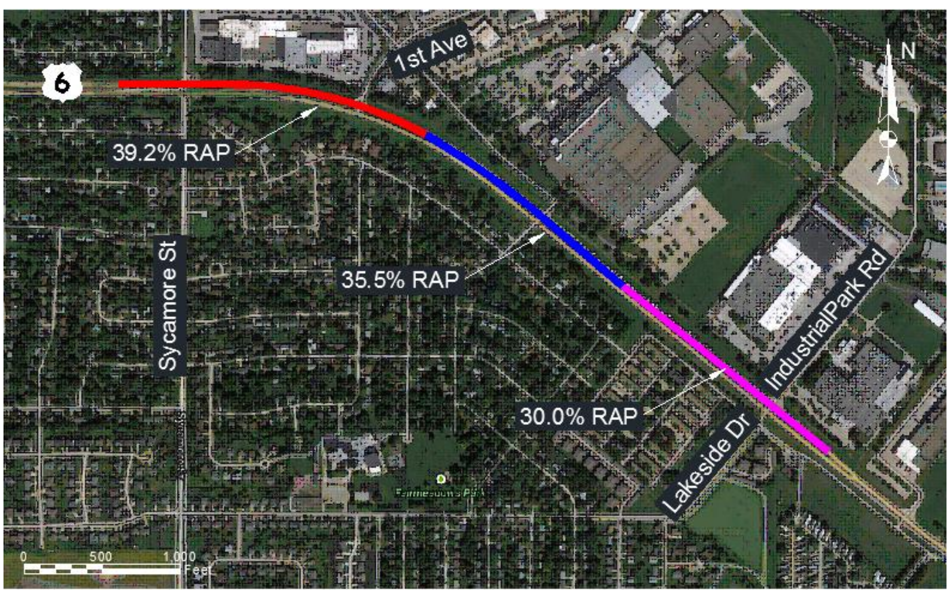

Figure 3-1: Layout of Test sections on Highway 6 in Iowa City

3.2 Binder Grade of Extracted Asphalt from Field Mixtures

To identify the effect of FRAP on the rutting potential of the virgin asphalt binder of PG 64-28, a Dynamic Shear Rheometer (DSR) test was performed on the asphalt binder extracted from field mixtures with varying FRAP amounts. It should be noted, however, that the extracted binder may not represent the actual blending level between virgin binder and binder from FRAP in the field because the laboratory extraction process would result in a better blending than the plant mixing process. As shown in Figure 3-2, the extracted binders from field mixtures with 30.0%, 35.5% and 39.2% FRAP met the minimum G*/sin delta value of 1 kPa for high temperatures of 76 ºC, 76 ºC, and 82 ºC, respectively. These high temperatures are two or three levels higher than the high temperature grade of 64 ºC for the virgin binder of PG 64-28. This result confirms that the similar level of stiffening in the original binder occurred due to 30.0% and 35.5% FRAP but more significant stiffening occurred with the 39.2% FRAP.

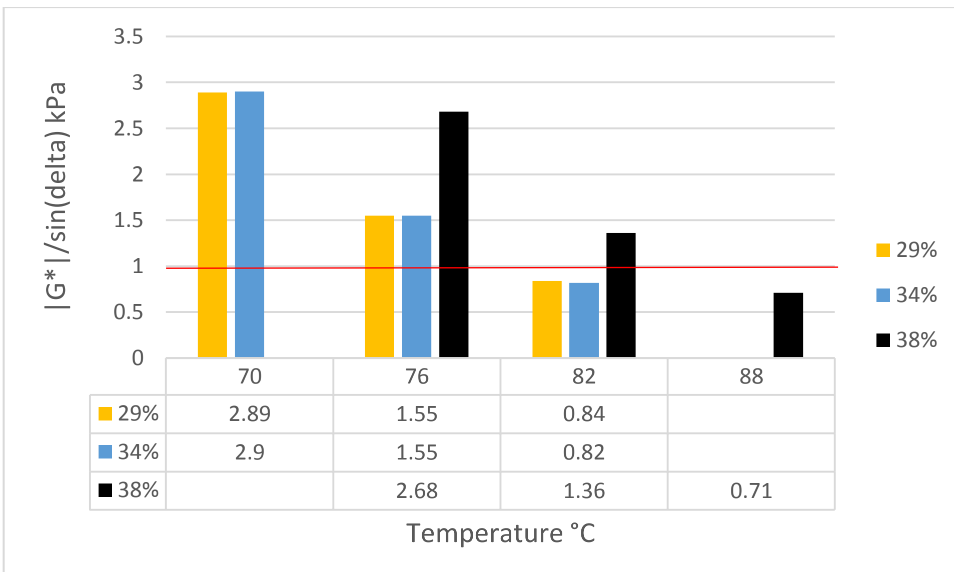

Figure 3-2: |G*| / sin (delta) vs temperature

To identify the effect of FRAP on the low-temperature cracking potential of the PG 64-28 virgin asphalt binder, the Bending Beam Rheometer (BBR) test was performed on asphalt binder extracted from field mixtures. As summarized in Table 3-1, the extracted binders from field mixtures with 30.0%, 35.5% and 39.2% FRAP met the minimum m-value of 0.300 and maximum stiffness value of 300 MPa for the low test temperatures of -12 ºC, -6 ºC, and -6 ºC, respectively. These temperatures are one or two levels higher than the low test temperature of -18 ºC of the virgin binder PG 64-28. This result confirms that the similar level of stiffening of the original binder has occurred for all FRAP contents.

Table 3-1: Bending Beam Rheometer Data

Temperature	-6 °C		-12 °C		-18 °C	
Percent RAP	Stiffness	m-Value	Stiffness	m-Value	Stiffness	m-Value
30.0%			201	0.301	354	0.271
35.5%	108	0.293	228	0.255		
39.2%	77.6	0.367	200	0.275		

Based on both DSR and BBR test results, the performance grade of extracted binders from the field mixtures with 30.0%, 35.5% and 39.2% FRAP can be classified as PG 76-22, PG 76-16, and PG 82-16, respectively. It can be concluded that the virgin binder of PG 64-28 used to build the test sections was significantly stiffened by the FRAP amounts due to the aged binder contained in the FRAP.

4 MIX DESIGN OF FIELD MIXTURES

The Superpave mix design was performed for a 10 million ESAL 1/2" mix with 30.0%, 35.5% and 39.2% FRAP materials by weight. Originally, PG 70-22 binder was specified for the proposed test sections. However, due to a high RAP content, a softer PG 64-28 binder was adopted (15). Percent binder replacements by RAP materials can be calculated as 20.1%, 24.7% and 29.0% for RAP materials of 30.0%, 35.5%, and 39.2% by weight using the following formula:

$$\%\,Binder\ Replacement = \frac{(\%\,of\ Binder\ Content\ in\ RAP \times \%\,of\ RAP\ in\ Mix)}{Total\ \%\,of\ Binder\ in\ the\ Mix} \times 100$$

4.1 High-RAP Mix Design Results

Table 4-1 summarizes the volumetric design criteria for the HMA 10 million ESAL 1/2" surface mixtures designed for this study. Volumetric properties were calculated at the optimum binder content of each mix and compared against these mix design criteria.

Table 4-1: Volumetric Mix Design Criteria

Mixture Property	Design Air Voids P_a (%)	Voids Filled w/ Asphalt VFA (%)	Voids in Aggregate VMA (%)	Film Thickness (μm)	Dust-Binder Ratio D:B	Maximum Dust Content (% -No. 200)
DOT Spec.	4.0	70 – 80	Min. 14.0	8.0 – 13.0	0.6 – 1.4	10.0

Table 4-2 summarizes both design and actual percentages of RAP by weight, optimum total binder contents, optimum virgin binder contents, and percentages of RAP by binder replacement. First, the optimum total binder content was calculated for each mix. Second, the amount of binder from FRAP was estimated and the remaining amount of virgin binder was derived. Finally, the percentage of FRAP by binder replacement was calculated. Due to a difficulty in weighing exact percentages of FRAP at the asphalt plant, actual percentages of FRAP used for building test sections were slightly increased.

Table 4-2: Percent RAP by Weight and by Binder Replacement

	% FRAP by weight					
	Design	Actual	Design	Actual	Design	Actual
% FRAP by Weight	29%	30.0%	34%	35.5%	38%	39.2%
Optimum Total AC	4.70%	4.80%	4.50%	4.49%	4.30%	4.38%
Optimum Virgin AC	3.70%	3.82%	3.40%	3.33%	3.10%	3.10%
% FRAP by Binder	20.1%	20.4%	24.7%	25.9%	29.0%	29.3%

Similarly, in Table 4-3, a summary of the mix design results for high RAP mixes with actual amounts of FRAP of 30.0% by weight (20.4% by binder replacement), 35.5% by weight (25.9% by binder replacement) and 39.2% by weight (29.3% by binder replacement). For each mix design, the optimum binder content was determined to produce 4% air voids for the 10 million ESAL 1/2" HMA mix. The volumetric properties of each mixture were determined at the optimum binder content and VMA, VFA, combined aggregate gradation, film thickness and dust-binder ratio were analyzed for each mix design.

Table 4-3: Volumetric Mix Design Results from Mixtures Used for Construction

Actual % FRAP by Weight	30.0%	35.5%	39.2%
% FRAP by Binder	20.4%	25.9%	29.3%
Optimum AC Content	4.80%	4.49%	4.38%
Max. Sp. Gr. (Gmm)	2.565	2.578	2.609
Core Sp. Gr. (Gmb)	2.497	2.507	2.549
Binder Sp. Gr. (Gb)	1.0183	1.0191	1.0196
Agg. Sp. Gr. (Gsb)	2.734	2.735	2.754
Water Absorp. (% Abs)	1.325	1.358	1.313
Effective Sp. Gr. (Gse)	2.778	2.778	2.81
Aggregate Surface Area	4.39	4.57	4.45
% Binder Abs. (Pba)	0.59	0.58	0.71
Effective Binder (Pbe)	4.24	3.94	3.67
Mix Design Criteria			
VMA (%)>14	13	12.5	11.5
70<VFA (%)<80	79.6	78.0	80.0
Dust Content<10	3.8	4.2	4.4
8<Film Thick<13	9.7	8.6	8.2
0.6<DB Ratio<1.4	0.92	1.14	1.2

Volumetric mix design results are presented in Figure 4-1. The fractionation method was effective in reducing the amount of fine aggregates from the original stockpile and thereby improving volumetric properties. These volumetric properties of the mixtures were significantly influenced by the optimum asphalt content of each mixture. Despite a reduced amount of fine aggregate and dust content due to a fractionation, all mix designs exhibited significantly lower optimum asphalt contents than a typical HMA mixture. The improvement of a mixture's volumetric properties was often offset by the lower optimum asphalt content resulting in a lower asphalt film thickness and a higher dust-binder ratio. The dust content was relatively low in the original RAP stockpile and, as can be seen from Figure 3-3, the mix designs met all of the Superpave mix design criteria except for the VMA. The VMA decreased as the amount of RAP materials increased because of less binder content and the increase in the dust proportion. The aggregates may not have been sufficiently crushed as the 10-million ESAL mix resulting in a low optimum binder content. The potential long-term impact of not meeting VMA requirement could lead to premature cracking and rutting due to low binder content, a large amount of dust from RAP materials and a low amount of crushed aggregates.

Figure 4-1: Volumetric results of constructed test sections

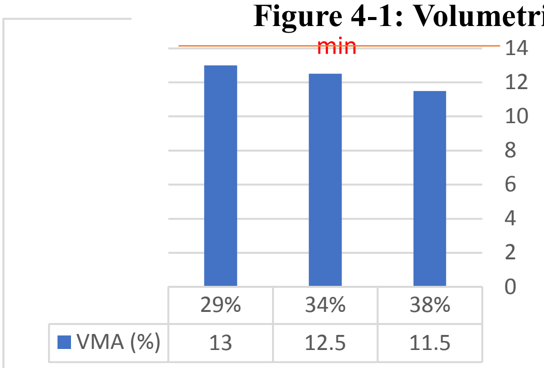

(a) Voids in the Mineral Aggregate (VMA)

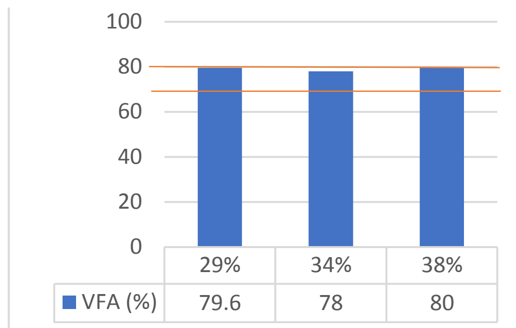

(b) Void filled with Asphalt (VFA)

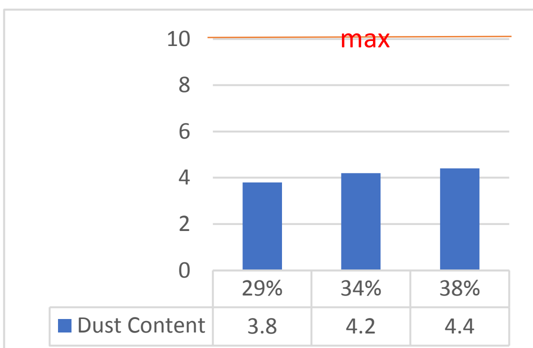

(b) Dust Content

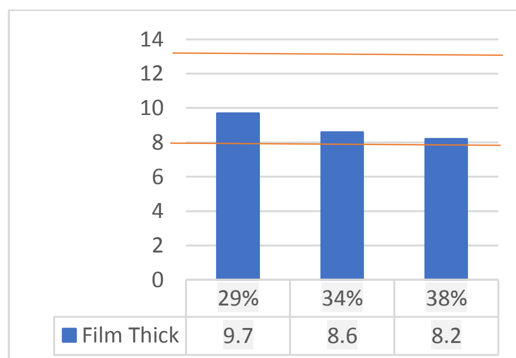

(d) Film Thickness

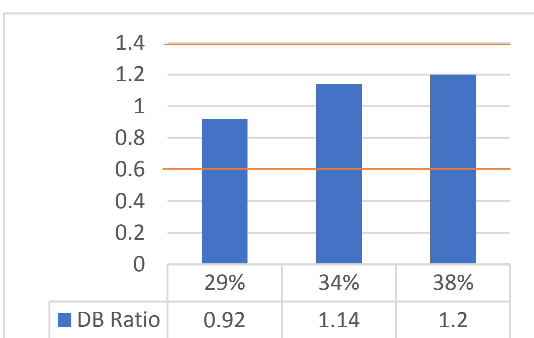

(e) Dust to Binder Ratio

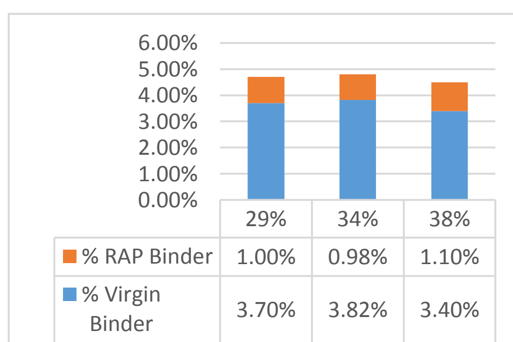

(f) Optimum Asphalt Content

5 LABORATORY EVALUATION OF FIELD MIXTURES

5.1 Hamburg Wheel Tracking Test

In order to evaluate the moisture susceptibility of field mixtures with varying FRAP amounts, the Hamburg Wheel Tracking (HWT) test was performed following the AASHTO T324 procedure and pictures of the HWT device can be seen in Figure 5-1. The HWT test applies a constant load of 685 N through a steel wheel in a water bath that is kept at 50 °C for the entirety of the test. In preparing the samples, the mixture was short-term aged for 4 hours at 135 °C (275 °F) followed by 2 hours at the compaction temperature of 145 °C (293 °F). The specimens were then prepared to a specific height of 61.5 mm and diameter of 150 mm. Finally, the specimens were conditioned at the test temperature of 50 °C for 30 minutes before the test begin. The HWT test was performed until it applied 20,000 passes or the rutting exceeded 20 mm. The stripping inflection point and stripping slope were used to identify the number of repetitions when the specimens failed due to a moisture damage.

Figure 5-1: Hamburg Wheel Tracking Device and Specimens ready for testing

Figure 5-2 shows the HWT test results for field mixtures with 30.0%, 35.5%, and 39.2% FRAP by weight. The target air voids for each sample was 6% which is considered a typical field density. All specimens exhibited excellent performance with very little rutting with no stripping inflection point in 20,000 passes. Therefore, given the limited test data, it can be concluded than the high-RAP field mixtures are not susceptible to moisture damage.

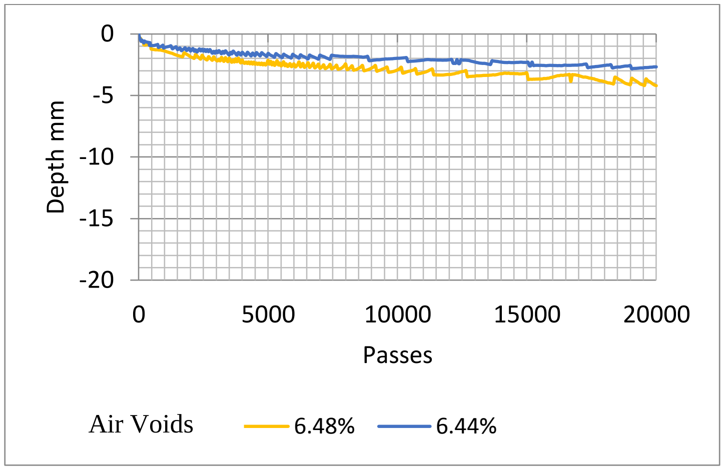

(a) 30.0% FRAP

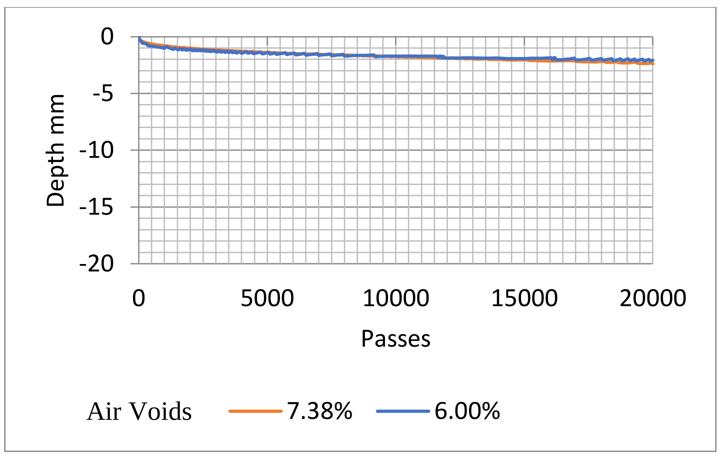

(b) 35.5% FRAP

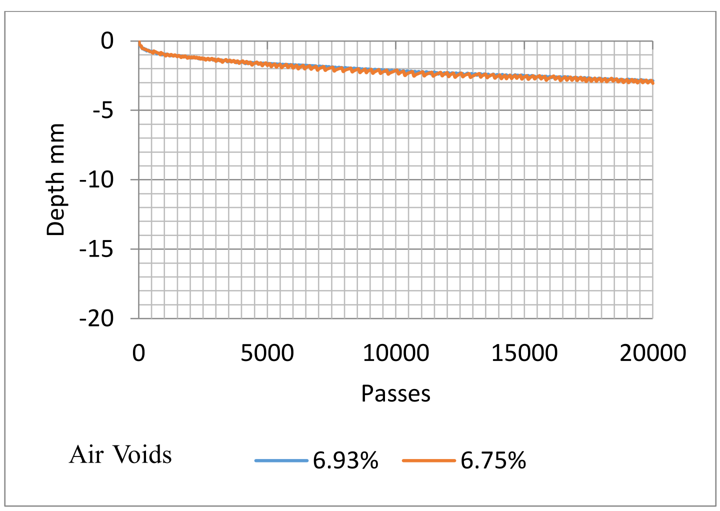

(c) 39.2% FRAP

Figure 5-2: Hamburg Wheel Tracking Test Results of High-FRAP Field Mixtures

5.2 Semi-Circular Bending Test

5.2.1 SCB Parameters and Measurements

Semi-circular bending (SCB) test was performed to evaluate the resistance of constructed asphalt in terms of low temperature cracking. The work of fracture was calculated by the area under load vs. load line displacement (P-u) curve shown in Figure 5-3. The test was stopped when the load drops significantly (vertical line in Figure 5-3). Total work of fracture (W_f) was calculated as the sum of the area under the left side of the vertical line (Mode 1) and right side of the vertical line (Mode 2). Mode 1 data were obtained from the test output file while Mode 2 data were estimated using the MATLAB software by extrapolating the tail of the loading curve (Buss and Williams 2013). A typical output data is presented in Figure 5-4.

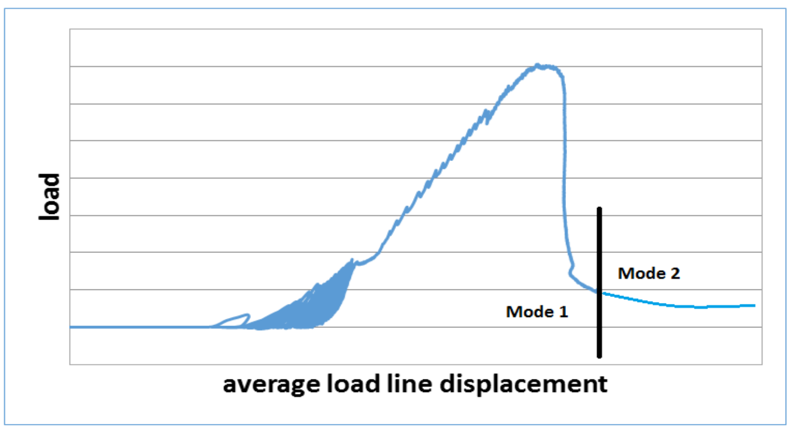

Figure 5-3: Typical SCB load vs. average load line displacement (P-u) curve

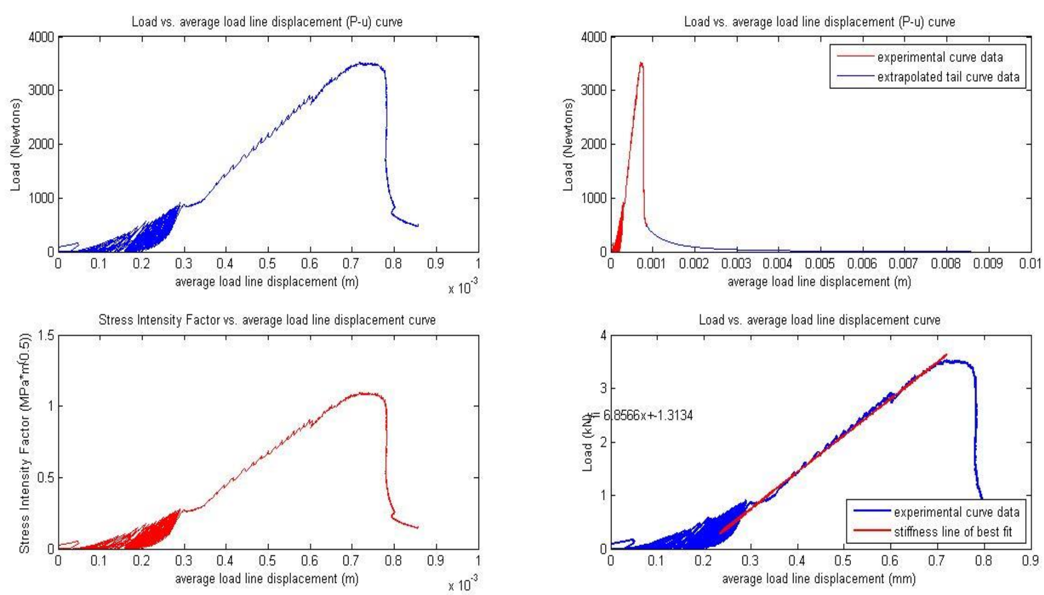

Figure 5-4: Typical output graph obtained from MATLAB software

The area under the curve can be calculated using the following equation:

$$W_{\text{mode 1}} = AREA = \sum_{i=1}^{n}(u_{i+1} - u_i) \cdot (P_i) + \frac{1}{2} \cdot (u_{i+1} - u_i) \cdot (P_{i+1} - P_i)$$

where,
Pi = applied load (N) at the *i* load step application,
Pi+1= applied load (N) at the *i* +1 load step application,
ui = average displacement at the *i* step, and
ui+1 = average displacement at the *i* +1 step.

$$W_{\text{mode 2}} = \int_{u_c}^{\infty} P d(u) = \int_{u_c}^{\infty} \frac{c}{u^2} d(u) = \frac{c}{u_c}$$

where,
u = integration variable equal to average displacement, and
u_c = average displacement value at which the test is stopped.

The work of total fracture is the sum of W_{mode1} and W_{mode2}:

$$W_f = W_{mode\ 1} + W_{mode\ 2}$$

Then, the fracture energy can be calculated using following equation:

$$G_f = \frac{W_f}{A_{lig}}$$

where,

G_f = fracture energy (J/m³)

A_{lig} = (r-a) * t

Fracture toughness (K_{IC}) is considered as the stress intensity factor at the critical load (P_c). The following equation can be used to calculate K_{IC}:

$$K_{IC} = Y_I . \sigma_c . \sqrt{\pi a}$$

$$\sigma_c = \frac{P_c}{2rt}$$

$$Y_I = 4.782 + 1.219\left(\frac{a}{r}\right) + 0.063\exp\left(7.045\left(\frac{a}{r}\right)\right)$$

where,

P_c = Peak load (MN)
r = sample radius (m)
t = sample thickness (m)
a = notch length (m)
Y_I = the normalized stress intensity factor (dimensionless)

5.2.2 Past Research about the SCB Test

To assess the low temperature cracking performance of warm mix asphalt (WMA), the SCB test was performed on WMA samples at three different temperatures (-24, -12 and 0°C) (Podolsky et al. 2014). As expected, the fracture energy increased as test temperature increased. However, as shown in Figure 5-5, the average fracture energy values seemed to be too high for all mixtures.

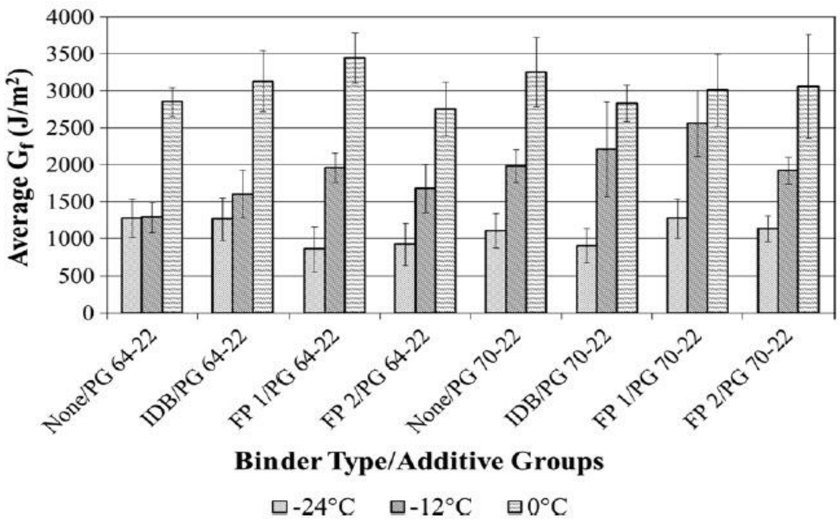

Fig 5-5: Fracture Energy Results (Podolsky et al. 2014)

As the test temperature increases, the fracture toughness is expected to increase. As can be seen from Fig 5-6, the fracture toughness increased when the test temperature was increased from -24 to -12°C but decreased when the test temperature increased from -12 to 0°C. The reduction in fracture toughness can be attributed by the transition from elastic to viscoelastic behavior when the temperature was increased from -12 to 0°C. As shown in Figure 5-7, the stiffness decreased as the test temperature was increased.

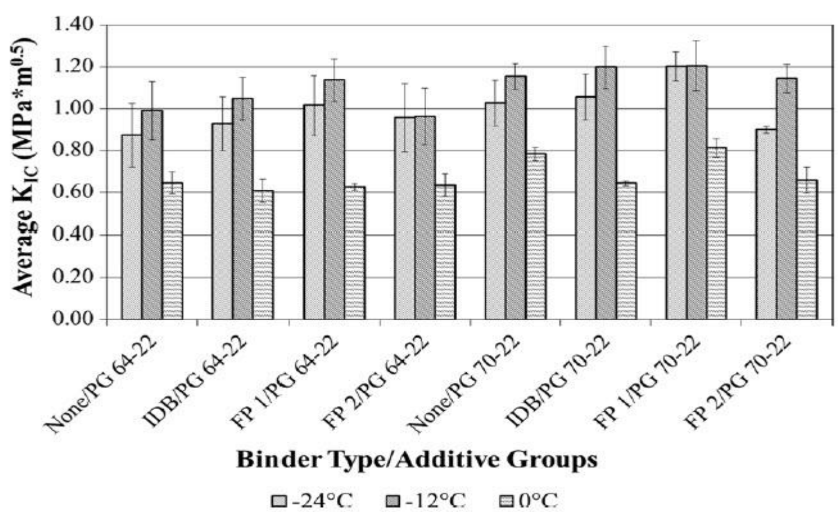

Fig 5-6: Fracture Toughness Results (Podolsky et al. 2014)

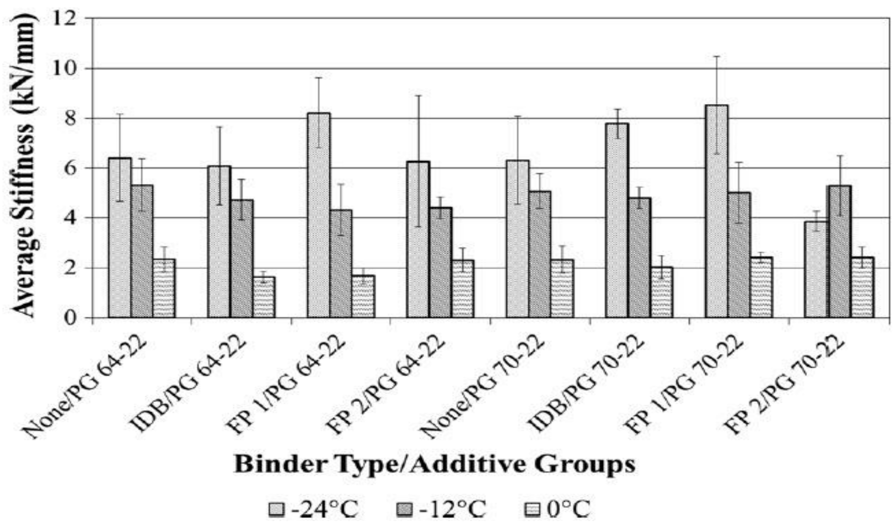

Fig 5-7 Fracture Stiffness Results (Podolsky et al. 2014)

Recently, West et al. (2013) has performed a comprehensive SCB test and the fracture energy and fracture toughness values are summarized for field mixtures from Utah, New Hampshire and Minnesota in Figures 5-8 through Figure 5-13, respectively. As can be seen from these figures, the fracture energy increased as the test temperature was increased. However, the fracture energy did not always decreased as the amount of RAP materials was increased. The average values of fracture energy were approximately 0.45, 0.6 and 0.3 kJ/m² for mixtures from New Hampshire, Utah and Minnesota, respectively. Contrary to the study done by Podolsky et al. (2014), the fracture toughness decreased as the temperature was increased.

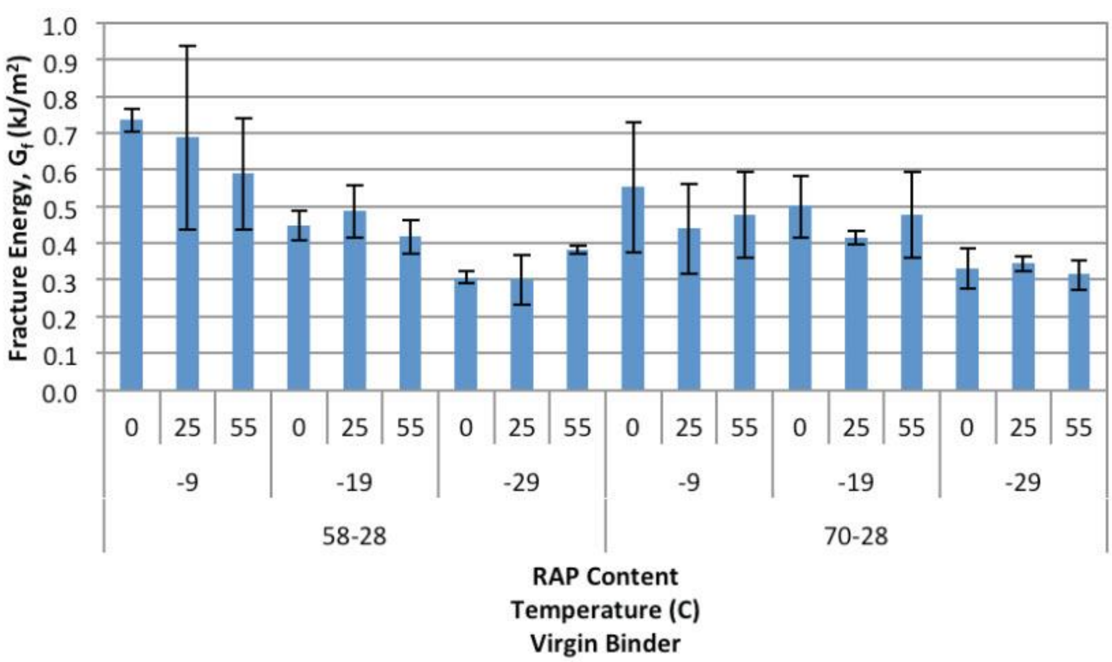

Fig 5-8: Fracture Energy Results for New Hampshire Mixes (West et al. 2013)

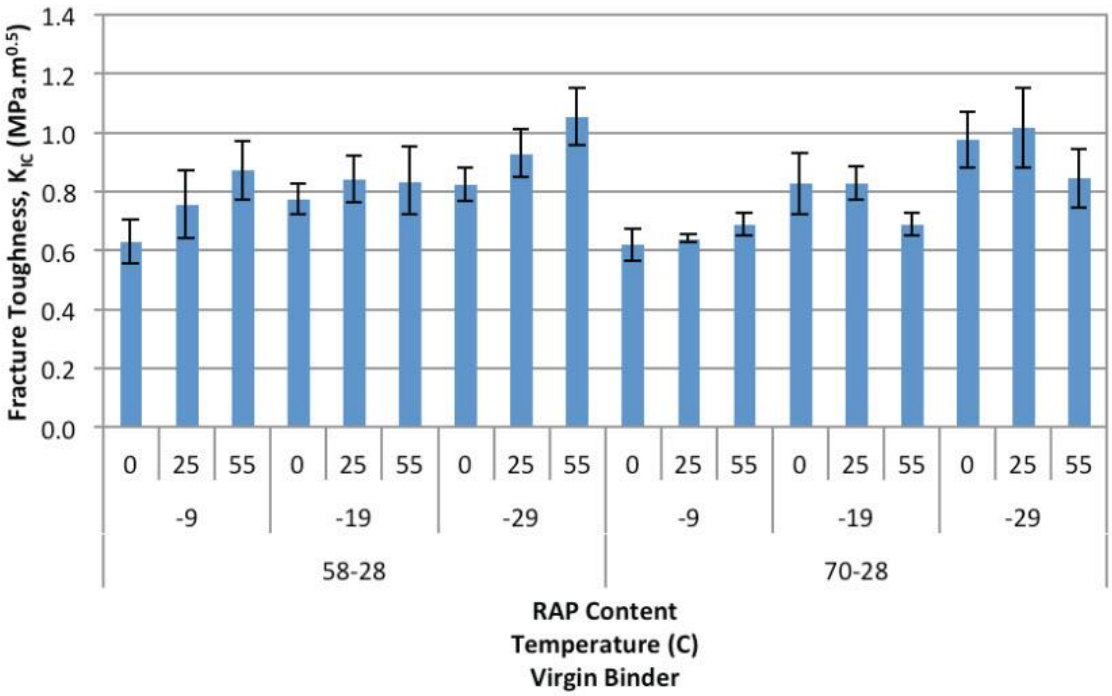

Fig 5-9: Fracture Toughness Results for New Hampshire Mixes (West et al. 2013)

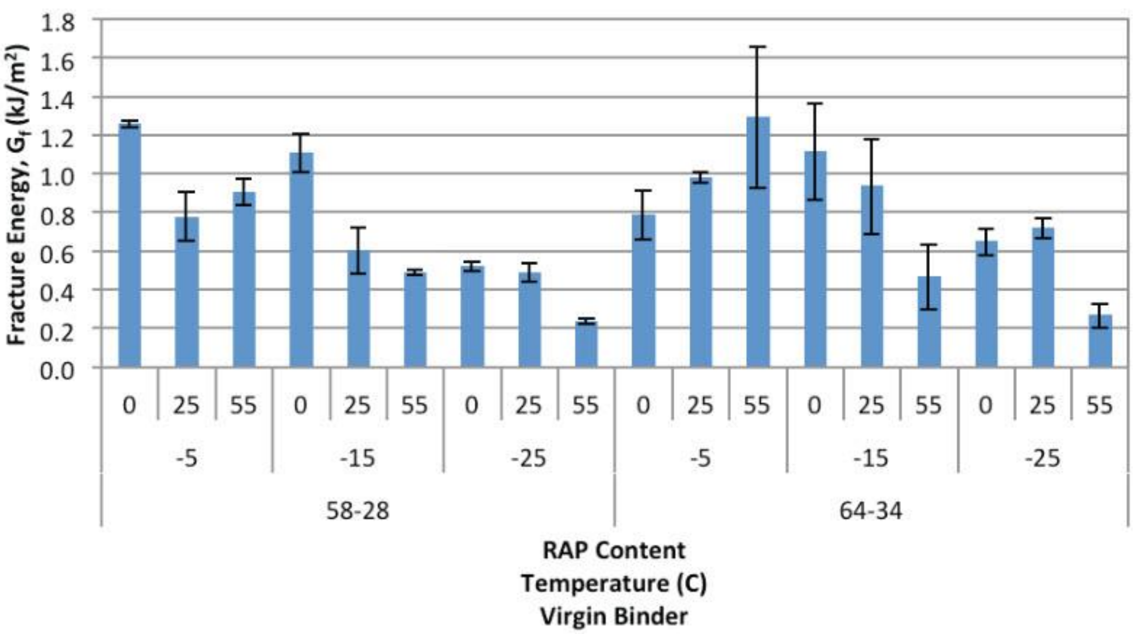

Fig 5-10: Fracture Energy Results for Utah Mixes (West et al. 2013)

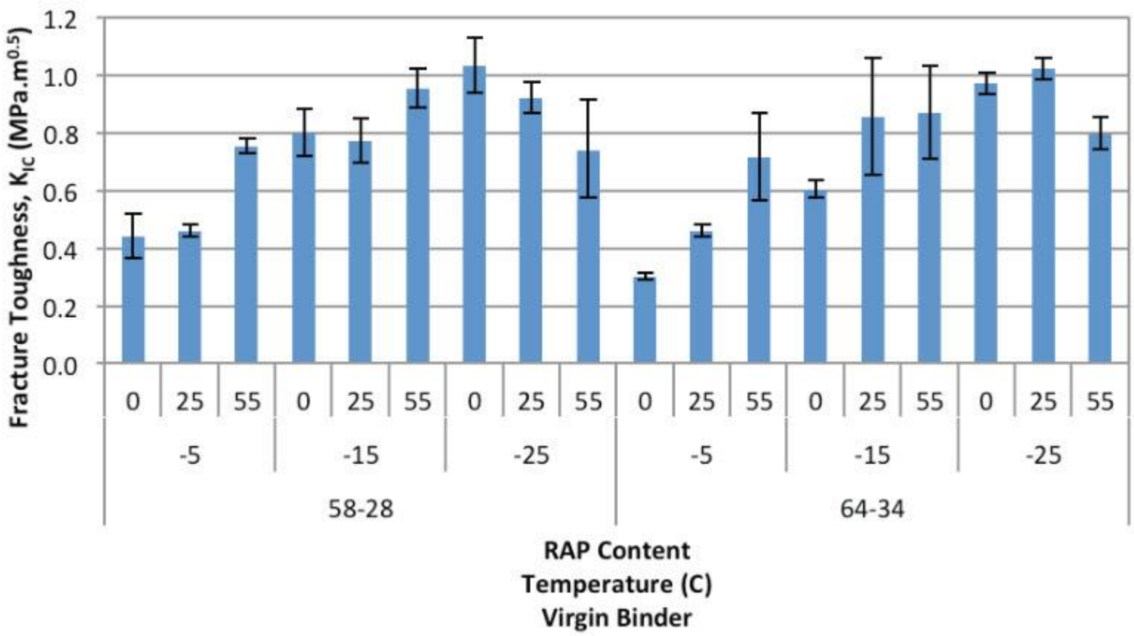

Fig 5-11: Fracture Toughness Results for Utah Mixes (West et al. 2013)

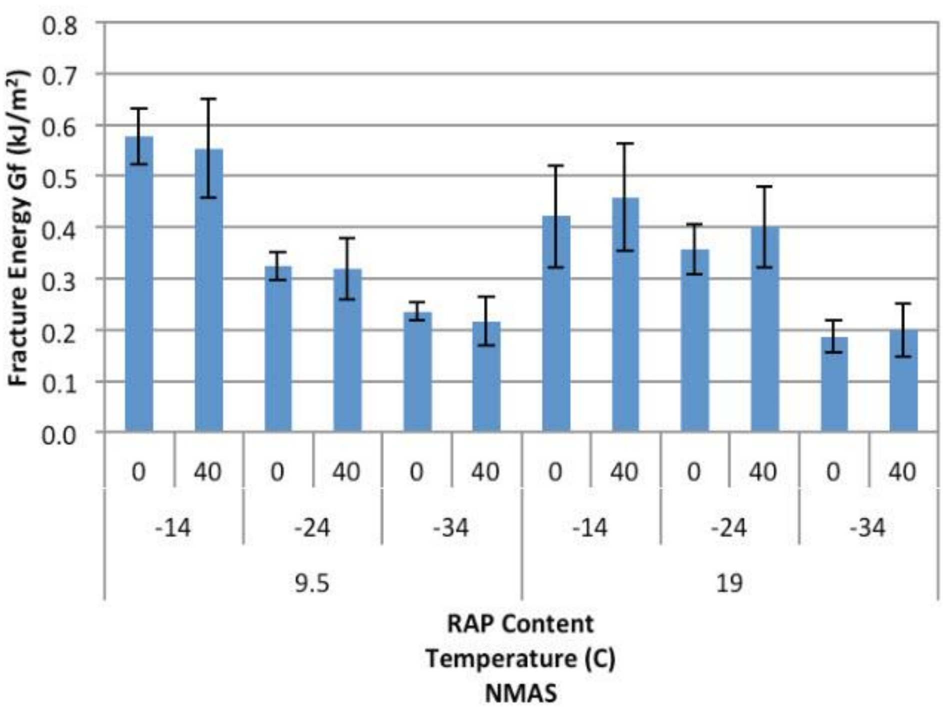

Fig 5-12: Fracture Energy Results for Minnesota Mixes (West et al. 2013)

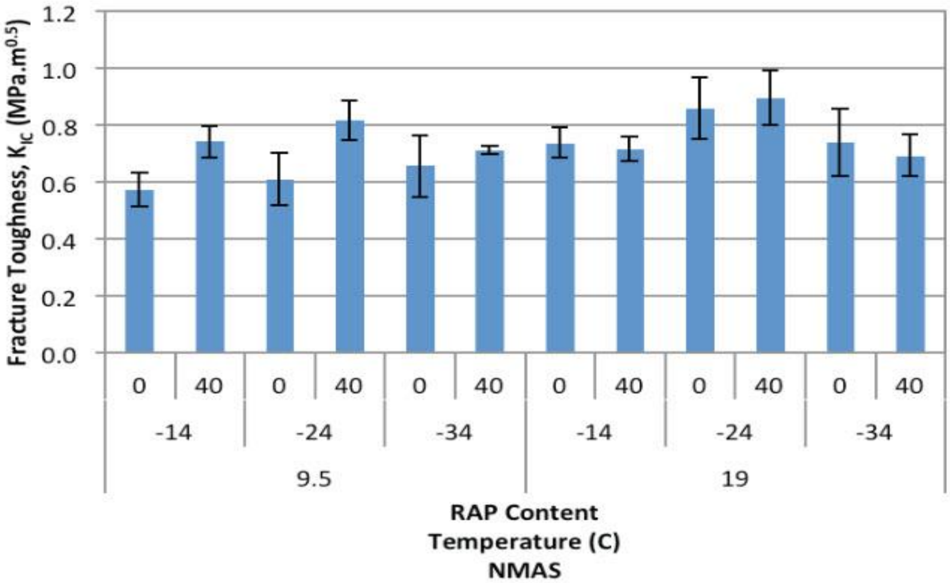

Fig 5-13: Fracture Toughness Results for Minnesota Mixes (West et al. 2013)

It is interesting to note that the control HMA mixtures tested by Podolsky (2014) exhibited a high level of fracture energy of 1200 J/m² at -24ºC whereas the control HMA mixture exhibited 500, 650 and 350 J/m² at -19 ºC , -25 ºC and -24 ºC, respectively, by West et al. (2013). Tang (2014) investigated the fracture properties of high-RAP mixtures and examined its variability with notch length, temperature and RAP content. Three different temperatures were selected for SCB test on samples with the RAP contents of 30%, 40% and 50%. As expected, the fracture energy increased as the test temperature was increased. However, the fracture energy values did not show a good correlation with the amounts of the RAP materials. As shown in Figure 5-14, the average values of fracture energy were 250, 300, 600 J/m² at -30, -20 and -10°C, respectively. As shown in Figure 5-15, fracture toughness increased as the test temperature was increased. However, there was no good correlation between the fracture toughness and RAP amounts. Overall, the average values of fracture toughness were 300, 650 and 2100 J/m² at -30, -20 and -10°C, respectively.

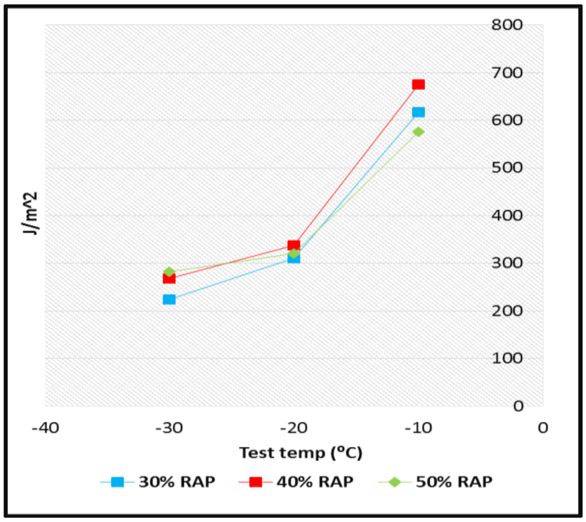

Fig 5-14 Fracture Energy for Three Percentages of RAP at Different Temperatures (Tang 2014)

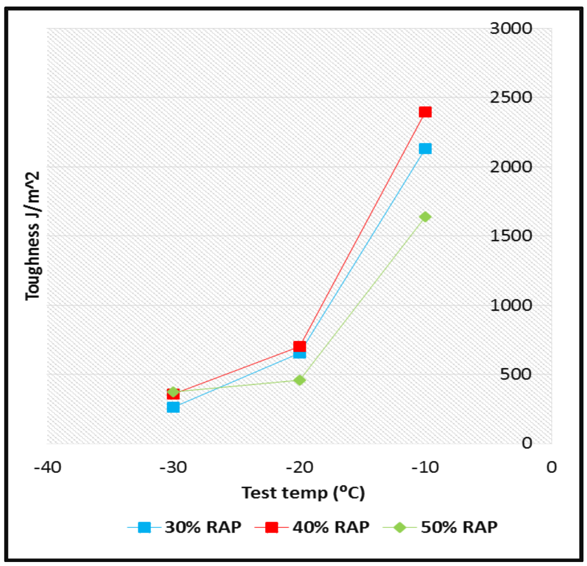

Fig 5-15 Fracture Toughness at Different RAP Contents and Temperatures (Tang 2014)

5.2.3 Results and Discussion

Fracture characteristics of field mixtures with varying RAP materials of 30.0%, 35.5%, and 39.2% by weight were measured using SCB test. For a given amount of RAP materials, three specimens were tested at each of two different test temperatures of -18 and -30 °C. The specimen and loading condition of SCB test are shown in Figure 5-16 and 5-17, respectively.

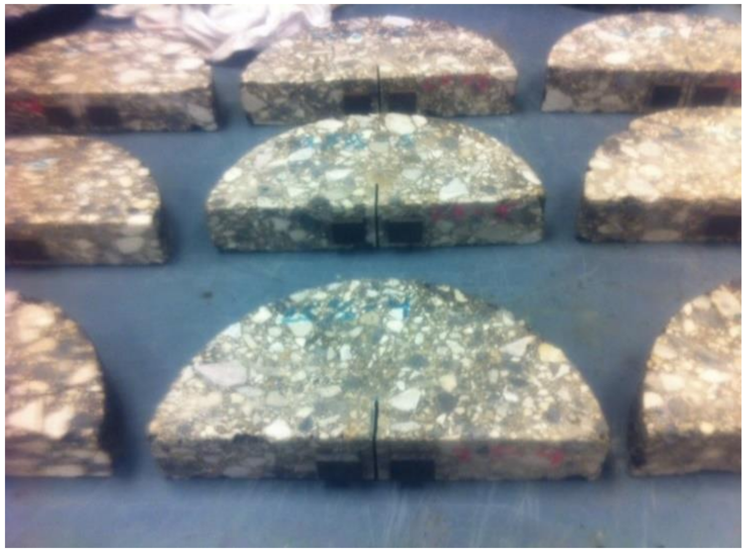

Figure 5-16: Specimens for SCB Test

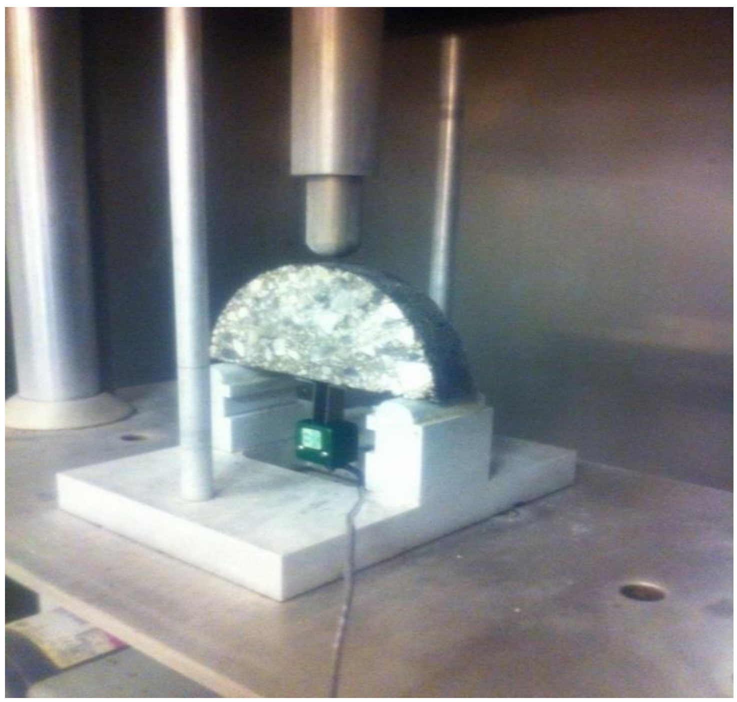

Figure 5-17: A Typical Specimen under SCB Test Machine

The SCB test results were used to calculate fracture work (W_f), fracture energy (G_f), fracture toughness (K_{IC}), and stiffness (S) using the MATLAB software. Table 5-1 summarizes the average value, the standard deviation and the covariance matrix computation (COV) of three specimens for each test parameter. As shown in Figure 5-18, most specimens exhibited COV values less than 25%, which indicates a satisfactory repeatability of the test procedure except the specimens with 39.2% RAP content. As can be seen from Figure 5-18, as the test temperature decreased, the fracture energy decreased and the stiffness increased. As the RAP amount increased, the stiffness increased and the fracture energy decreased.

Table 5-1: Semi-Circular Bending Test Results

Temp.	RAP	t (mm)			W_f (J)					G_f (J/m^2)					K_{IC} (Mpa*m$^{0.5}$)				Stiffness (kN/mm)		
C	%	t	Avg.	STDEV	Wf	Wtail	Avg.	STDEV	COV(%)	Gf	Gftail	Avg.	STDEV	COV(%)	kIC	Avg.	STDEV	COV(%)	S	Avg.	STDEV
		25.2			1.45	0.39				957.20	258				0.93				3.98		
	30	25.6	25.4	0.21	1.16	0.31	1.20	0.08	7.09	688.43	203	765	56	7.3	0.99	0.97	0.03	3.49	6.00	5.05	1.02
		25.3			0.9866	0.22				649.95	146				0.99				5.18		
		25.3			1.05	0.26				688.42	168				0.96				5.88		
-18	35.5	25.2	25.4	0.21	1.01	0.25	1.20	0.08	6.39	670.55	165	789	49	6.2	0.97	1.01	0.08	8.06	6.21	5.73	0.58
		25.6			1.547	0.39				1007	251				1.10				5.09		
		25.3			0.83	0.22				545.34	142				0.98				7.78		
	39.2	25.1	25.5	0.47	1.0785	0.21	0.92	0.01	1.41	716.16	141	610	6	0.9	1.08	0.97	0.12	11.96	8.40	7.36	1.31
		26			0.855	0.24				567.42	151				0.85				5.89		
		24.4			0.95	0.23				645.73	159				1.21				8.87		
	30	24.6	24.7	0.31	1.31	0.34	1.24	0.09	7.59	886.80	227	834	61	7.3	1.17	1.08	0.18	16.43	5.75	5.69	3.21
		25			1.45	0.42				968.18	280				0.88				2.46		
		25.4			0.74	0.95				484.47	624				0.85				6.72		
-30	35.5	25.7	25.5	0.15	1.59	2.73	1.13	1.25	110.25	1030.00	-	738	292	39.5	0.97	0.91	0.06	6.78	3.36	4.92	1.69
		25.5			1.07	0.32				700.04	212				0.91				4.67		
		24.4			0.90	0.24				616.62	165				1.06				7.13		
	39.2	25.3	25.0	0.49	0.62	0.91	0.81	0.37	45.56	411.08	-	541	22	4	1.17	1.11	0.05	4.93	13.82	9.98	3.45
		25.2			0.90	0.30				593.84	196				1.10				8.98		

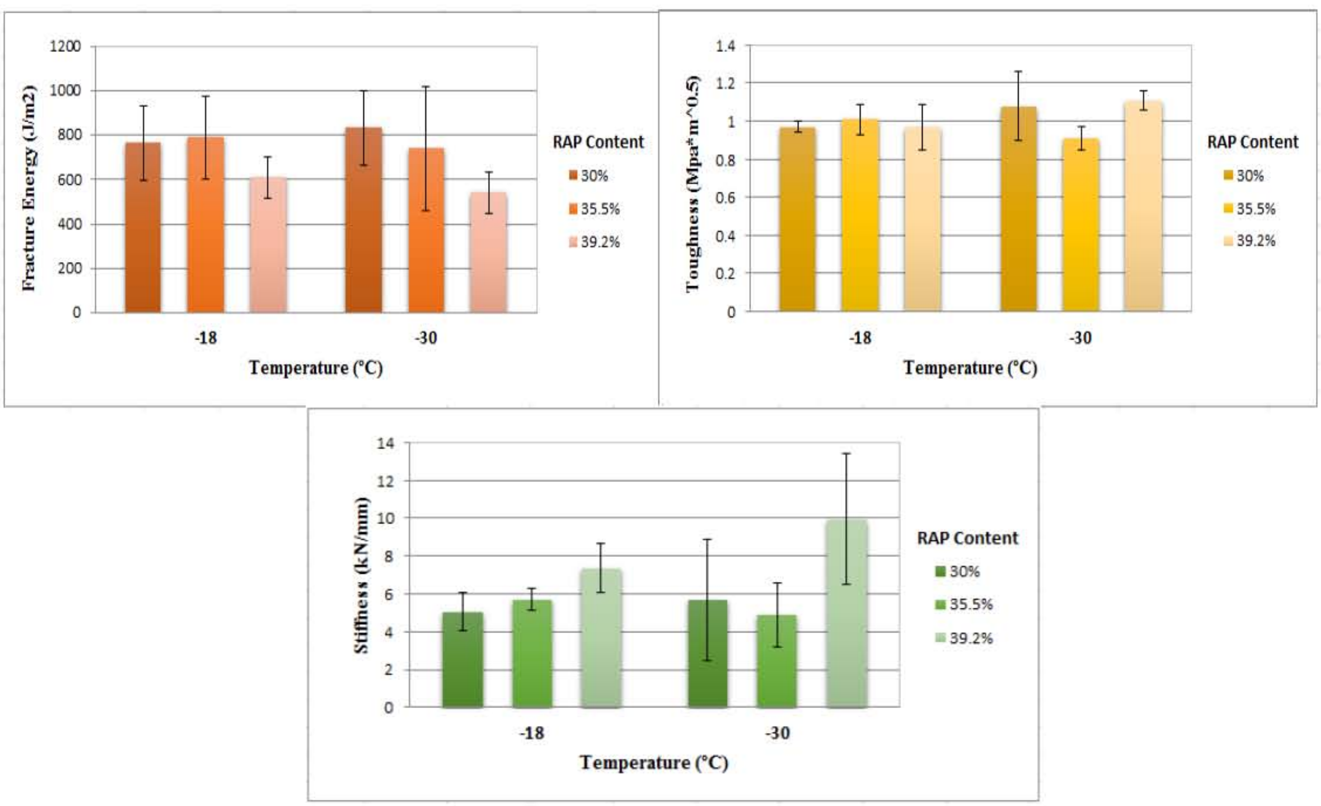

Figure 5-18: Plot of SCB test parameters against RAP content

6 FIELD PERFORMANCE OF HIGH RAP PAVEMENTS

On the night of September 8, 2013, three test sections, each with approximately 0.35 mile, were constructed with a 1.5-inch thick surface layer on top of a 1.5-inch thick intermediate layer. The traffic level for the test sections is approximately 13,100 ADT with 24% trucks. As summarized in Table 6-1, the average bulk-specific gravity of cores from the test sections with 30.0%, 35.5% and 39.2% FRAP were 2.446, 2.422 and 2.460, resulting in air voids of 4.7%, 6.0% and 5.7%, respectively. Since the target air voids are 6.0% +/- 2.0%, all three sections met the field air void requirement.

6.1 Condition Survey of Test Sections

To evaluate the short-term performance of the test sections, a pavement condition survey was performed on May 29, 2014, about 8 months after construction. Throughout the test section, no distress was observed other than transverse cracking. As shown in Figure 6-1, a dominant distress type was reflective joint cracking, which were typically spaced at about twenty feet intervals. This extensive transverse cracking was likely caused by a combined effect of underlying deteriorated concrete pavement joints and one of the coldest Iowa winters on the record with many freeze and thaw cycles. Length and severity of transverse cracks were measured and their results are summarized in Table 6-2. Considering RAP differences as the only known factor for the evaluation of three test sections, the test section with 39.2% FRAP performed the best followed by the test sections with 35.5% and 30.0% FRAP. Based on the limited field data, it can be concluded that as the FRAP amount is increased; the amount of transverse cracking is decreased.

Table 6-1: Density and Air Voids of Field Cores

Core	Station	Gmb	% of Gmm	Pa (%)	Thickness (in.)
1	268+95	2.430	94.7	5.3	1.625
2	268+72	2.488	97.0	3.0	1.375
3	265+07	2.448	95.4	4.6	1.375
4	262+63	2.426	94.6	5.4	1.750
5	259+52	2.447	95.4	4.6	1.750
6	256+10	2.435	94.9	5.1	1.750
Average		2.446	95.3	4.7	1.604
Stan. Dev.		0.023	0.9	0.9	0.184

a. 30.0% FRAP Field Core Data

b. 35.5% FRAP Field Core Data

Core	Station	Gmb	% of Gmm	Pa (%)	Thickness (in.)
1	252+63	2.433	94.4	5.6	1.500
2	247+19	2.436	94.5	5.5	1.500
3	245+53	2.382	92.4	7.6	1.625
4	242+27	2.426	94.1	5.9	1.625
5	239+36	2.444	94.8	5.2	1.625
6	238+02	2.413	93.6	6.4	1.625
Average		2.422	94.0	6.0	1.583
Sta Dev.		0.022	0.9	0.9	0.065

c. 39.2% FRAP Field Core Data

Core	Station	Gmb	% of Gmm	Pa (%)	Thickness (in.)
1	234+65	2.407	92.3	7.7	1.625
2	229+88	2.467	94.6	5.4	1.750
3	229+33	2.487	95.3	4.7	1.500
4	216+40	2.441	93.6	6.4	1.500
5	213+89	2.463	94.4	5.6	1.250

6	209+39	2.493	95.6	4.4	1.250
Average		2.460	94.3	5.7	1.479
Stan. Dev.		0.032	1.2	1.2	0.200

(a) Low (b) Medium (c) High

Figure 6-1: Examples of low, medium, and high severity cracking

Table 6-2: Transverse Cracking Developed in Three Test Sections

Severity	30.0% FRAP	35.5% FRAP	39.2% FRAP
High	0 ft	12 ft	0 ft
Medium	288 ft	216 ft	84 ft
Low	411 ft	315 ft	366 ft
Total	699 ft	531 ft	450 ft
Section Length	1841 ft	1787 ft	1787 ft
Per 100’ Sta.	38.0 ft	29.7 ft	25.2 ft

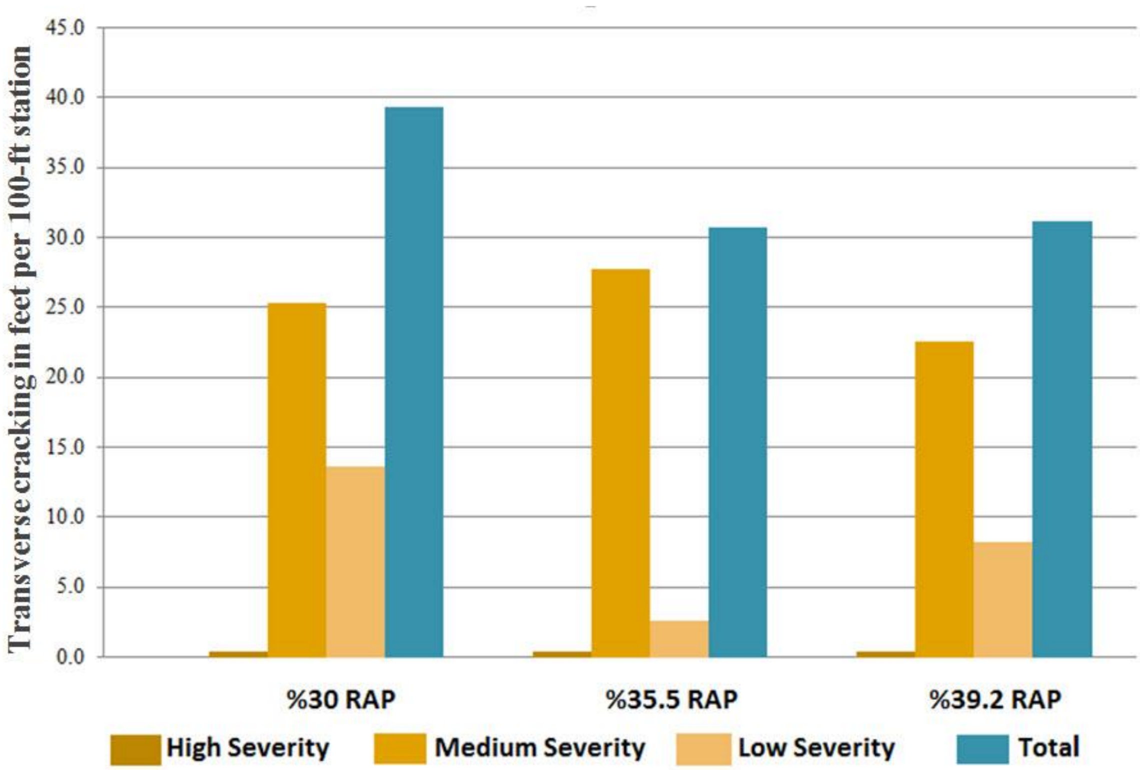

Figure 6-2: Length of Reflective Cracking Measured from Each Test Section

7 SUMMARY AND CONCLUSION

This report discusses efforts to evaluate test sections constructed with varying amounts of RAP materials. First, the sieve analysis of the classified RAP materials identified the distribution of aggregates and binder associated with RAP materials retained on each sieve. RAP materials were then fractionated by removing fine RAP materials passing the 5/16" sieve. Mix designs were performed on mixtures with target amounts of Fractionated RAP (FRAP) materials of 30%, 35% and 40% by weight and they passed all volumetric design criteria except VMA. It can be concluded that the fractionation was effective in improving volumetric properties of HMA mixtures with a high RAP content.

Three test sections with actual amounts of 30.0%, 35.5% and 39.2% FRAP were constructed on Highway 6 in Iowa City, Iowa and the average field densities measured from the cores were 95.3%, 94.0%, and 94.3%, respectively, which met density requirement of 94% ± 2.0%. Superpave binder tests were then performed in order to determine the binder grade of extracted binder from field mixtures with varying FRAP amounts. Based on the limited test results, it can be concluded that as the RAP material is increased, both high and low temperatures of performance grade of the asphalt binder are also increased.

Field mixtures were compacted in the laboratory to evaluate the moisture sensitivity using a Hamburg Wheel Tracking (HWT) device and rut depths after 20,000 passes were less than 3mm for all three test sections. To evaluate the low temperature cracking resistance of asphalt mixtures, the Semi-Circular Bending (SCB) test was performed on specimens with 30.0%, 35.5% and 39.2% RAP materials by weigh at two different temperatures of -18°C and -30°C. As expected, the fracture energy decreased when the test temperature decreased. As the test temperature decreased, the fracture energy decreased and the stiffness increased. As the RAP amount increased, the stiffness increased and the fracture energy decreased.

Finally, a condition survey was performed on the test sections with varying FRAP contents to evaluate their relative performances in the 8 months after construction. The test section with 39.2% FRAP performed the best followed by 35.5% FRAP and 30.0% FRAP. As the FRAP amount was increased from 30.0% to 39.2%; the amount of transverse cracking decreased by approximately by 34%.

7.1 Proposed Phase 3 Study

The phase 2 study demonstrated a potential of using RAP materials up to 40% by weight. However, to further improve the low temperature cracking behavior, the use of the rejuvenator should be considered. The main objective the phase 3 study is to develop a set of tools to evaluate various rejuvenators for its effectiveness in chemically restoring the maltenes that would be compatible with the original asphaltenes. The proposed research should be performed in four tasks.

First, a diffusion of rejuvenators in hardened asphalt should be examined using Fourier Transform Infrared Spectroscopy (FTIR). The absorbance differences for different wavenumbers can be used to assess the diffusion rate of various rejuvenators. X-Ray Fluorescence technology (XRF) should be also considered for evaluating the elements in the diffused interface. Atomic Force Microscopy (AFM) should be used to measure the nanoscale surface morphology and mechanical properties of the extracted asphalt with various rejuvenators. How the rejuvenator diffuse with the extracted asphalt should be investigated to identify the rejuvenation mechanism of extracted asphalt. Both topographical and mechanical properties should be simultaneously captured by recording instantaneous force curves as the AFM probe approaches and retracts from the diffused surface of the extracted asphalt with various rejuvenators. The dissipated energy and elastic vs. damping ratio of diffused interface should be measured at nanoscale pixel level and, as a result, a signature map should be obtained.

Second, the effect of the rejuvenators on the PG grade of hardened asphalt should be evaluated. A set of Superpave binder tests including Multiple Stress Creep Recovery (MSCR) test should be performed on hardened asphalt with and without rejuvenators. Different types and dosages of the rejuvenator should be added to the hardened asphalt to evaluate their effects on the properties of hardened asphalt.

Third, the moisture susceptibility of high Recycled Asphalt Materials (RAM) mix with and without rejuvenators should be evaluated using HWT device. The effects of rejuvenators on the low-temperature characteristics of high-RAM mixtures should be examined using the Disk-Shaped Compact Tension Test (DCT). Dynamic modulus and flow number of high RAM mixtures should be measured using Asphalt Material Performance Tester (AMPT). Fatigue performance of specimens with and without rejuvenators should be also evaluated.

Fourth, to evaluate field performance of high RAM mixtures with and without select rejuvenator(s), test sections should be constructed. The field loose mixtures and cores should be tested using HWT, DCT, AMPT testing equipment and compared against the test results of laboratory mixtures. The short-term condition survey should be performed on the test sections with or without select rejuvenator(s).

8 REFERENCES

Al-Qadi, I. L., M. A. Elseifi and S. H. Carpenter, “Reclaimed Asphalt Pavement – A Literature Review,” Research Report FHWA-ICT-07-001, Illinois Center for Transportation, March 2007.

Bennert, T., J. S. Daniel, and W. Mogawer. Strategies for Incorporating Higher RAP Percentages: Review of Northeast States Implementation Trials. Presented at 93rd Annual Meeting of the Transportation Research Board, Washington, D.C., 2014.

Boriack, P., S. W. Katicha, and G. W. Fintsch. A Laboratory Study on the Effect of High RAP and High Asphalt Binder Content on the Stiffness, Fatigue Resistance and Rutting Resistance of Asphalt Concrete. Presented at 93rd Annual Meeting of the Transportation Research Board, Washington, D.C., 2014.

Buss, A., & Williams, R. C. (2013). Investigation of Warm Mix Asphalt for Iowa Roadways–Phase II.

Diefenderfer, S. and N. Harikrishnan. Evaluation of High RAP Mixture Production, Construction, and Properties. Presented at 93rd Annual Meeting of the Transportation Research Board, Washington, D.C., 2014.

Huang, B., G. Li, D. Vukosavljevic, X. Shu and B. K. Egan, “Laboratory Investigation of Mixing Hot-Mix Asphalt with Reclaimed Asphalt Pavement,” Transportation Research Record: Journal of the Transportation Research Board, No. 1929, Washington, D.C., 2005, pp. 37-45.

Iowa DOT, “Supplemental Specifications for Recycled Asphalt Pavement (RAP),” effective on January 20, 2010.

Maupin, G. W., S. D. Diefenderfer and J. S. Gillespie, “Evaluation of Using Higher Percentages of Recycled Asphalt Pavement in Asphalt Mixes in Virginia,” VTRC 08-R22, VTRC, June 2008.

McDaniel, R. S. and R. M. Anderson, “Recommended Use of Reclaimed Asphalt Pavement in the Superpave Mix Design Method: Technicians Manual,” NCHRP Report 452, TRB, Washington, D.C., 2001.

McDaniel, R. S., H. Soleymani and A. Shah, “Use of Reclaimed Asphalt Pavement (RAP) Under Superpave Specifications,” FHWA/IN/JRRP-2002/6, Purdue University, 2002.

NCAT, “Asphalt Technology News,” Vol. 22, No. 1, Spring 2010.

Podolsky, J. H., Buss, A., Williams, R. C., & Cochran, E. (2014). Comparative performance of bio-derived/chemical additives in warm mix asphalt at low temperature. *Materials and Structures*, 1-13.

Stephens, J. E., J. Mahoney, and C. Dippold, “Determination of the PG Binder Grade to Use in a RAP Mix,” Report No. JHR 00-278, Connecticut Department of Transportation, 2001.

Tang, S. (2014). Evaluate The Fracture and Fatigue Resistances of Hot Mix Asphalt Containing High Percentage Reclaimed Asphalt Pavement (RAP) Materials at Low and Intermediate Temperatures. *Iowa State Thesis*.

Udelhofen, G., “High RAP Design Works,” Asphalt Contractor, January 2007.

Udelhofen, G., “Overland Park Successfully Constructs First FRAP Project,” Asphalt Contractor, May 2010.

West, R. C., Willis, J. R., & Marasteanu, M. O. (2013). *Improved mix design, evaluation,*

and materials management practices for hot mix asphalt with high reclaimed asphalt pavement content: Transportation Research Board.
Wisconsin DOT, "Section 460 Hot Mix Asphalt Pavement," 2010 Standard Specifications, effective in December, 2009.

Appendix A: SCB Output Graphs

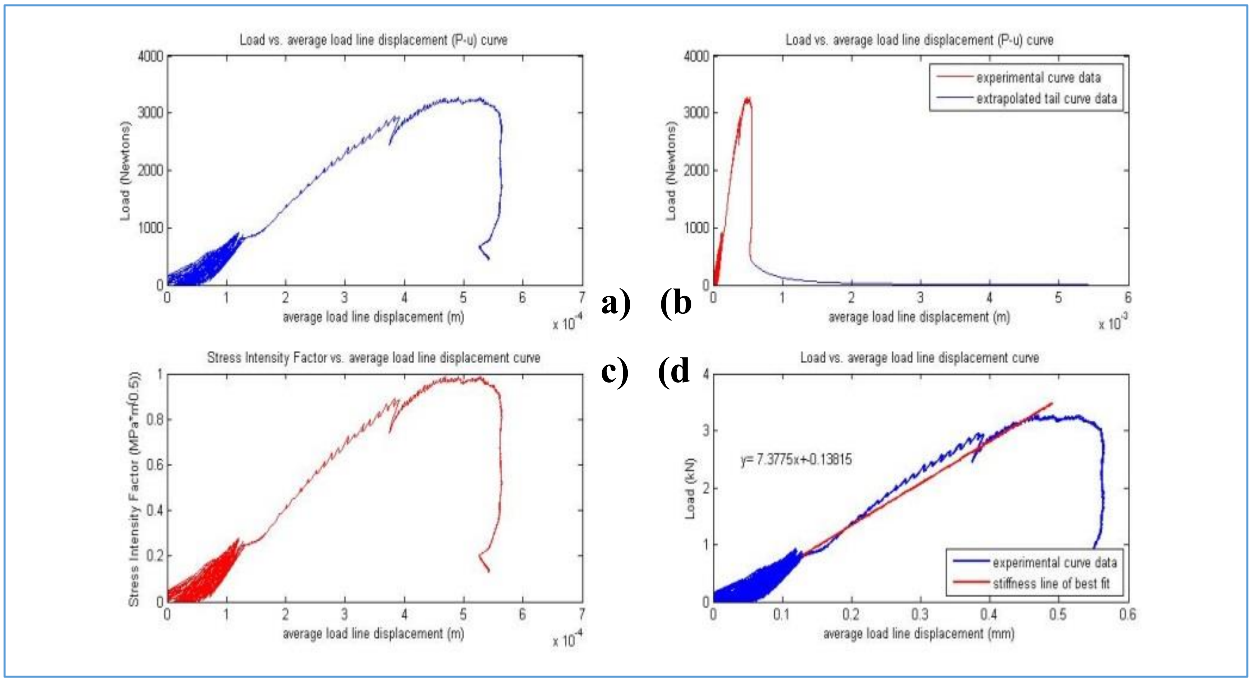

Sample #1) Load-Displacement plot for 30% RAP @ -18 ºC
a) Load-Displacement, b) tail-end modeling c) stress intensity factor, d) stiffness

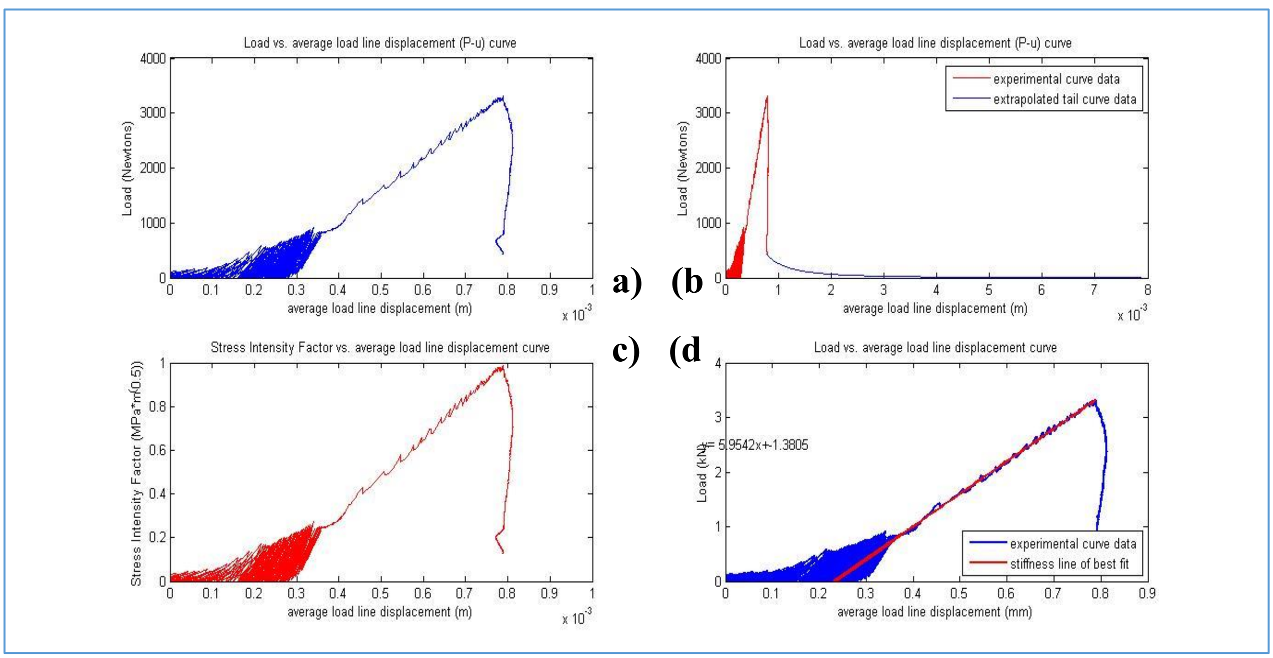

Sample #2) Load-Displacement plot for 30% RAP @ -18 ºC
a) Load-Displacement, b) tail-end modeling c) stress intensity factor, d) stiffness

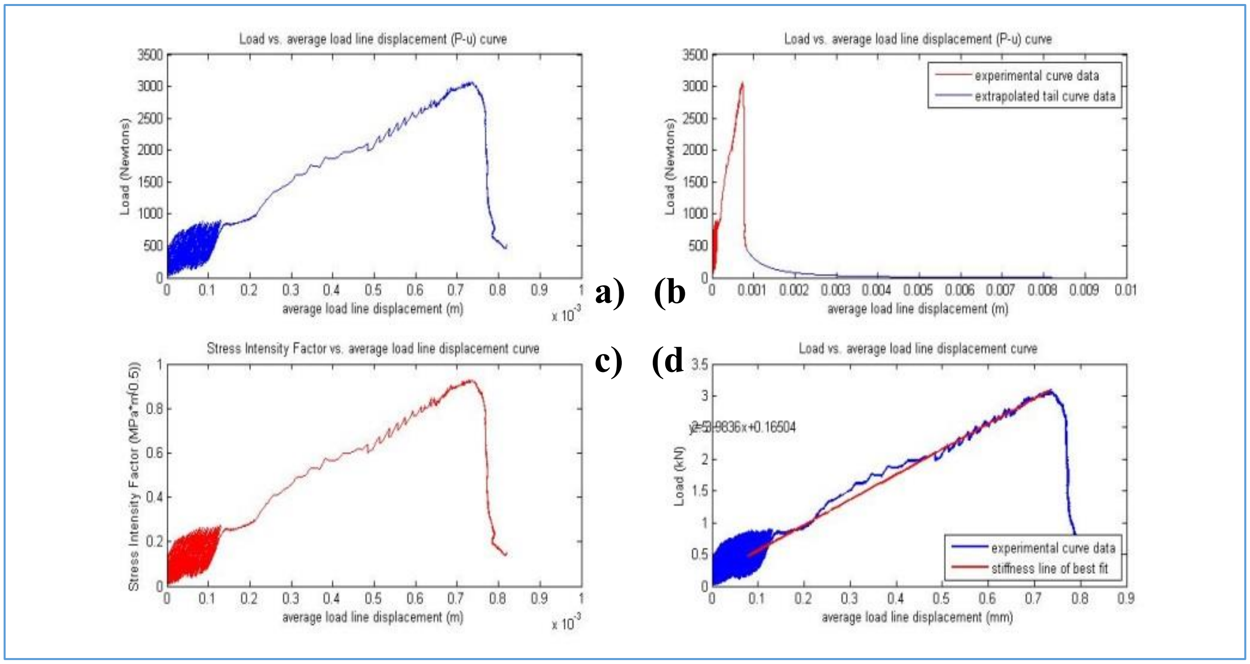

Sample #3) Load-Displacement plot for 30% RAP @ -18 ºC

a) Load-Displacement, b) tail-end modeling c) stress intensity factor, d) stiffness

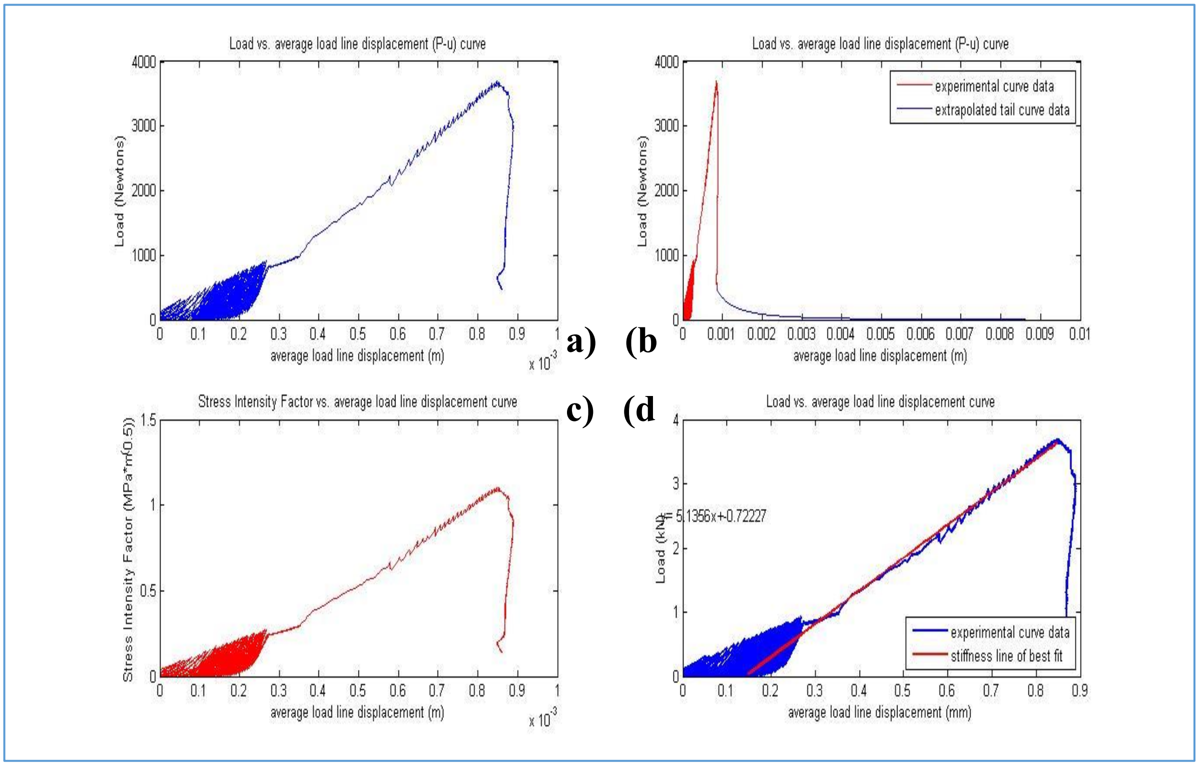

Sample #1) Load-Displacement plot for 35.5% RAP @ -18 ºC

a) Load-Displacement, b) tail-end modeling c) stress intensity factor, d) stiffness

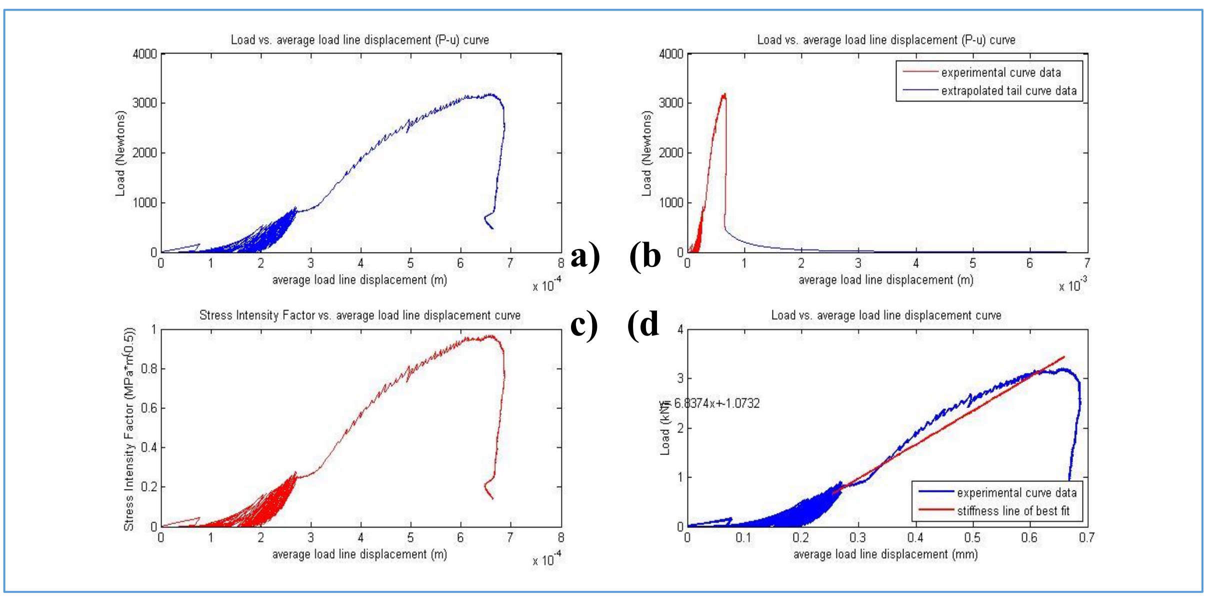

Sample #2) Load-Displacement plot for 35.5% RAP @ -18 ºC

a) Load-Displacement, b) tail-end modeling c) stress intensity factor, d) stiffness

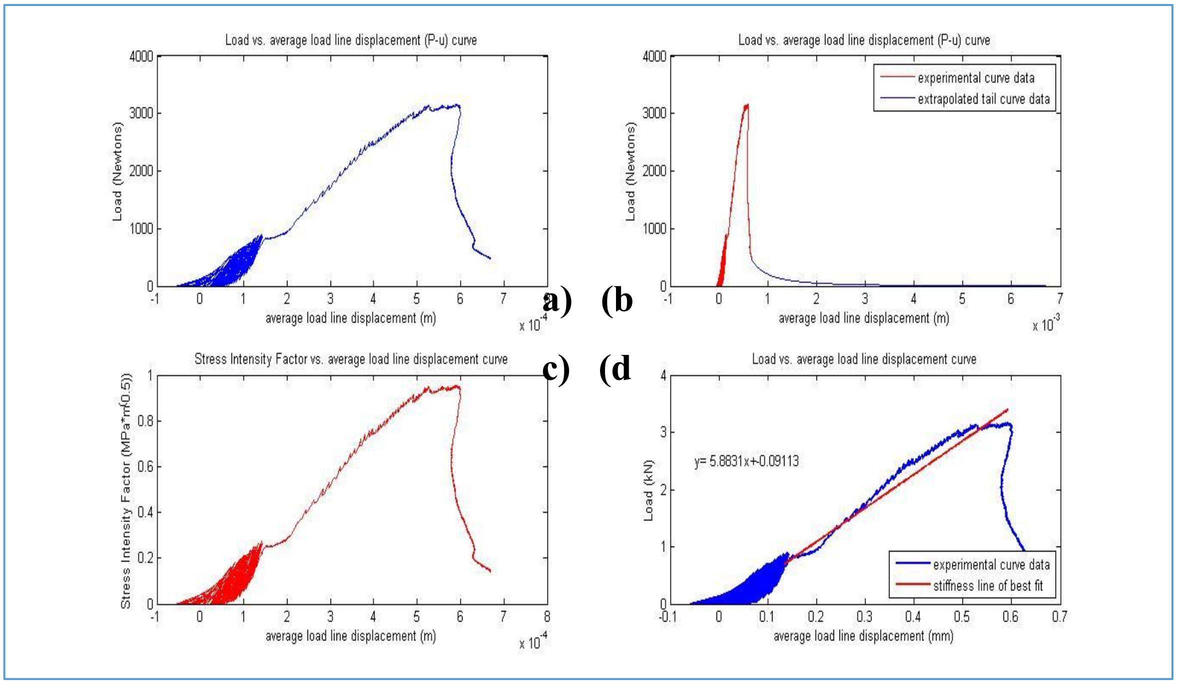

Sample #3) Load-Displacement plot for 35.5% RAP @ -18 ºC

a) Load-Displacement, b) tail-end modeling c) stress intensity factor, d) stiffness

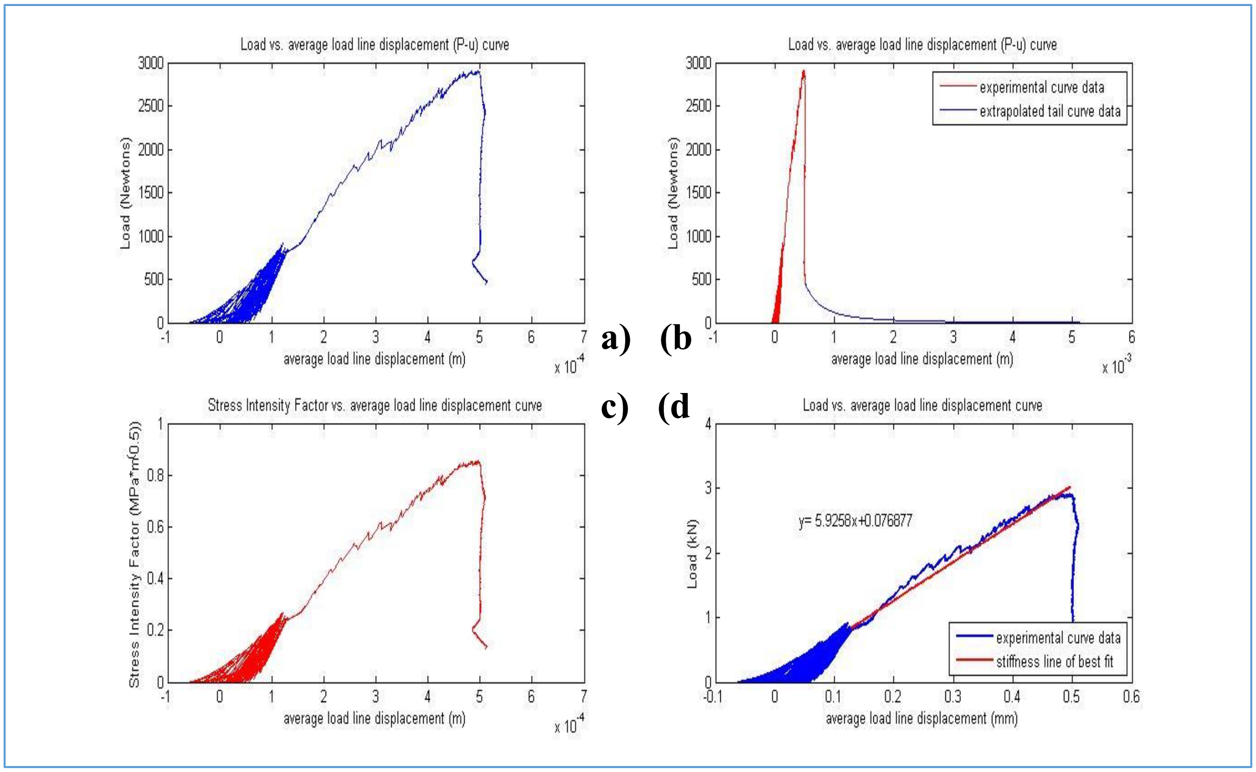

Sample #1) Load-Displacement plot for 39.2% RAP @ -18 ºC

a) Load-Displacement, b) tail-end modeling c) stress intensity factor, d) stiffness

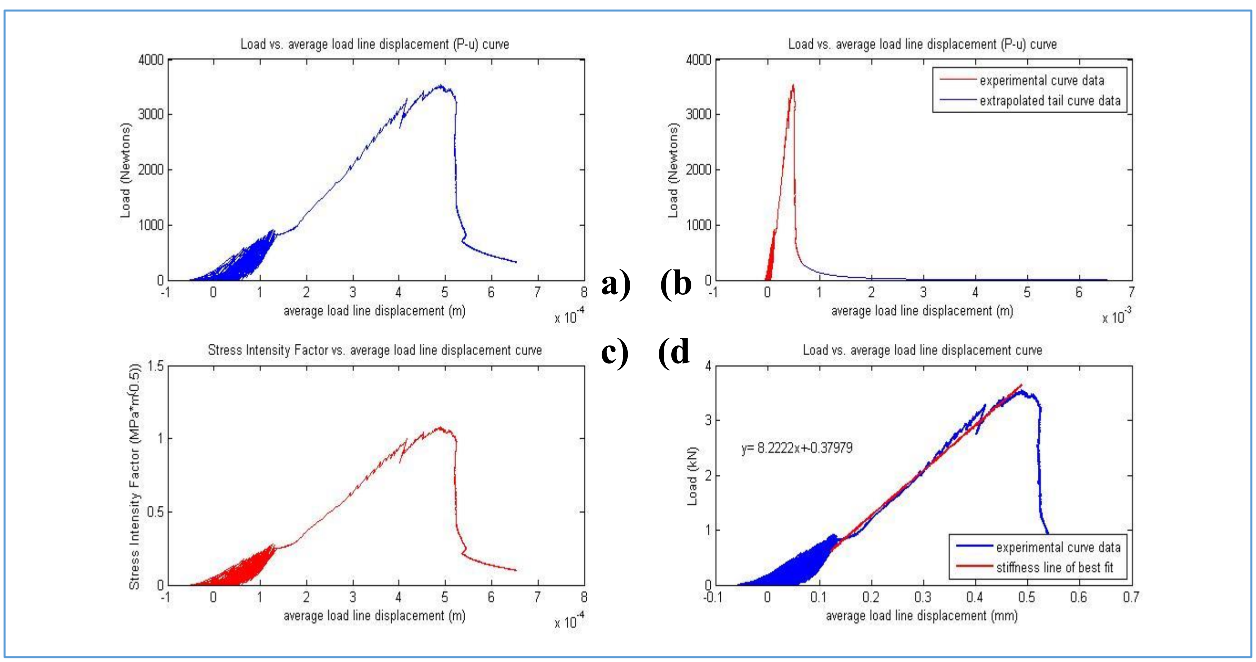

Sample #2) Load-Displacement plot for 39.2% RAP @ -18 ºC

a) Load-Displacement, b) tail-end modeling c) stress intensity factor, d) stiffness

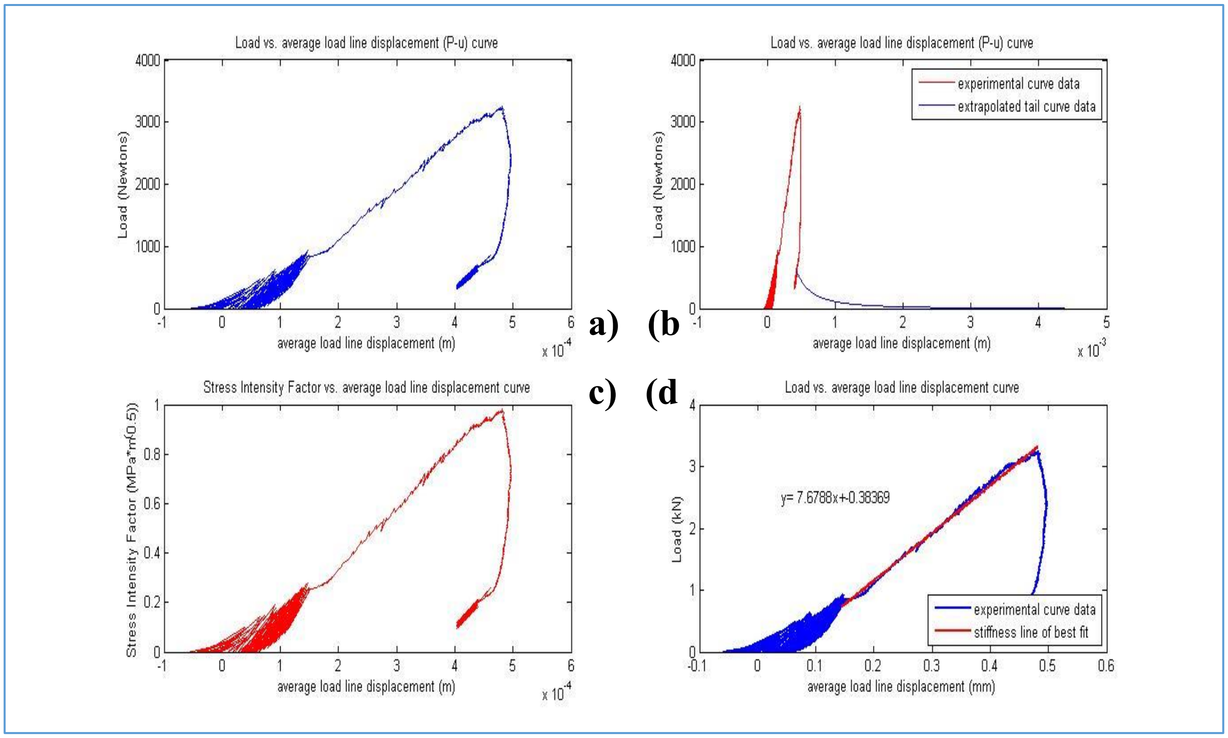

Sample #3) Load-Displacement plot for 39.2% RAP @ -18 ºC

a) Load-Displacement, b) tail-end modeling c) stress intensity factor, d) stiffness

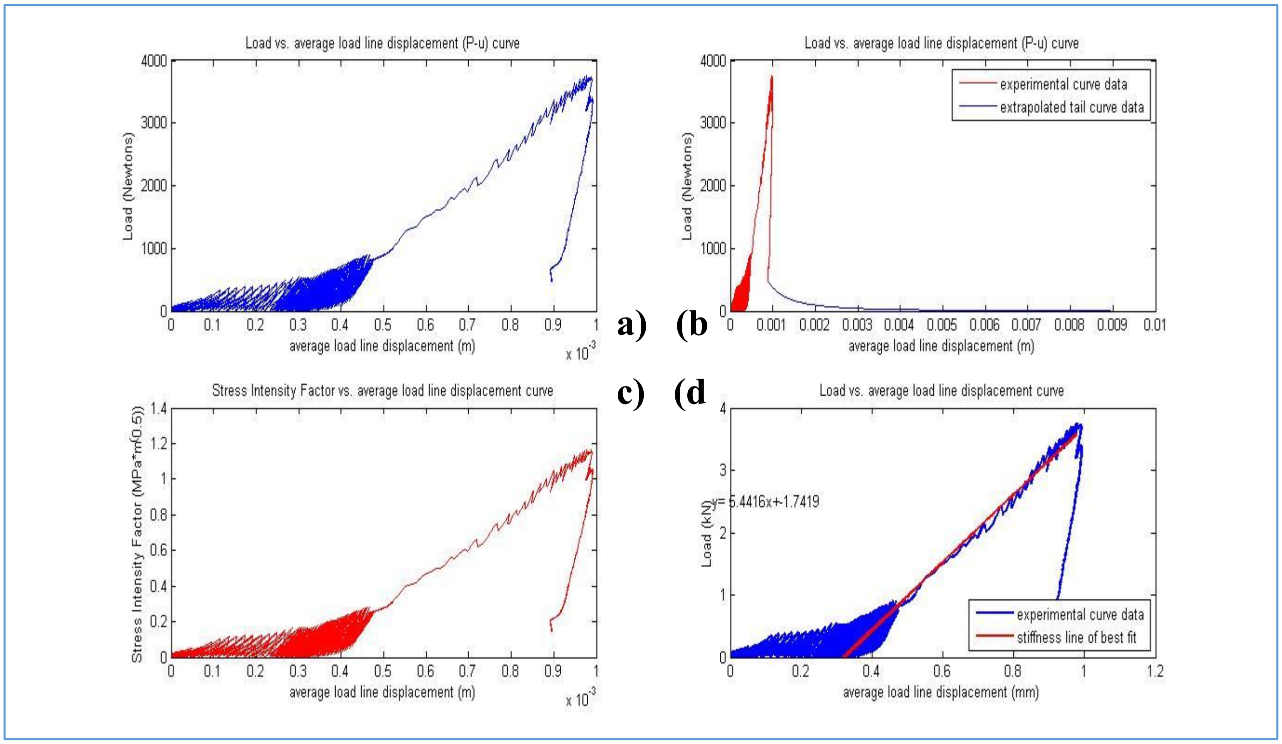

Sample #1) Load-Displacement plot for 30% RAP @ -30ºC

a) Load-Displacement, b) tail-end modeling c) stress intensity factor, d) stiffness

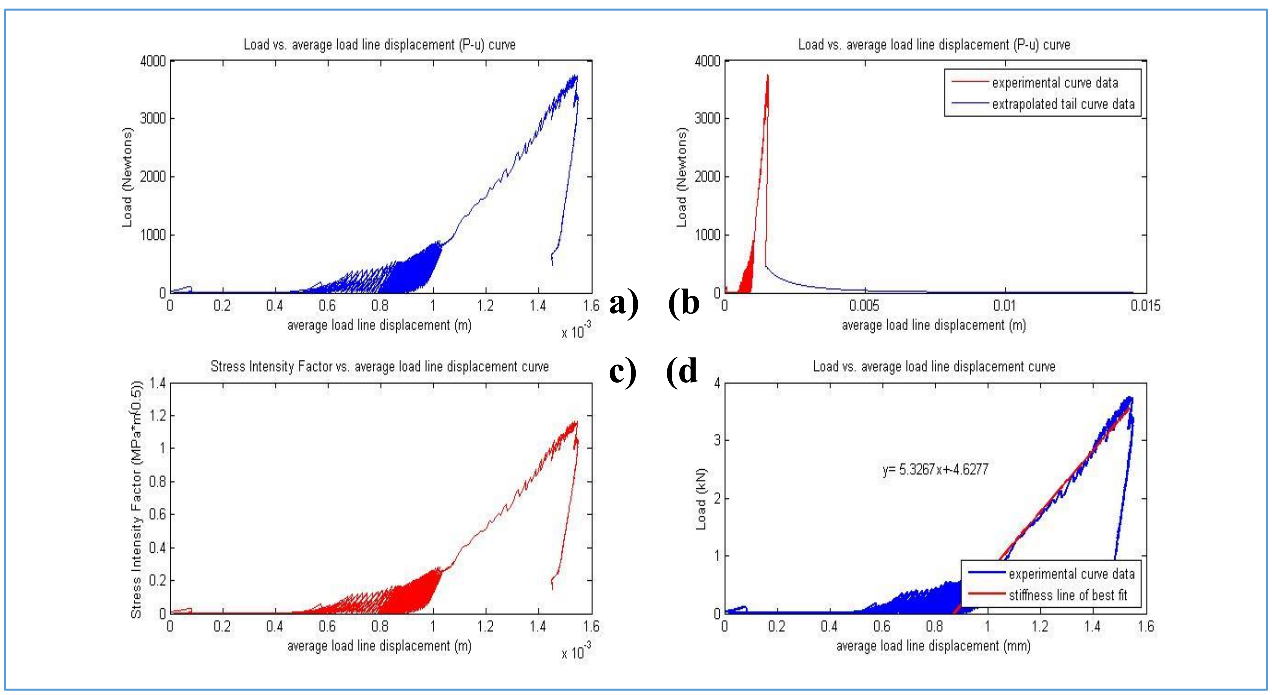

Sample #2) Load-Displacement plot for 30% RAP @ -30ºC

a) Load-Displacement, b) tail-end modeling c) stress intensity factor, d) stiffness

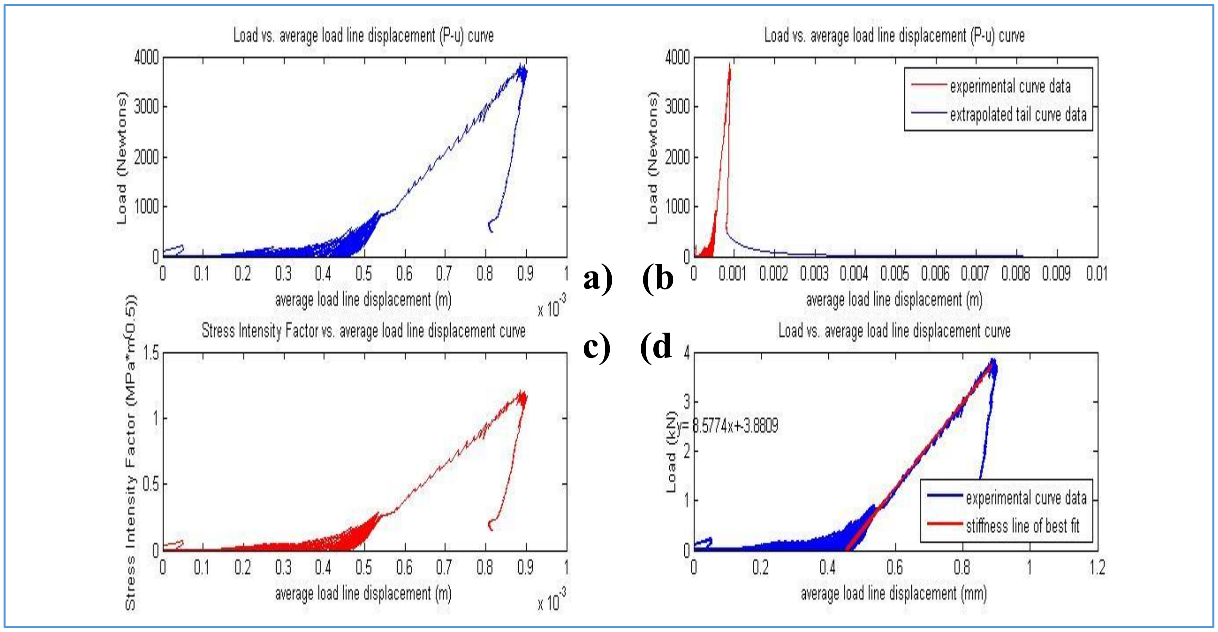

Sample #3) Load-Displacement plot for 30% RAP @ -30ºC

a) Load-Displacement, b) tail-end modeling c) stress intensity factor, d) stiffness

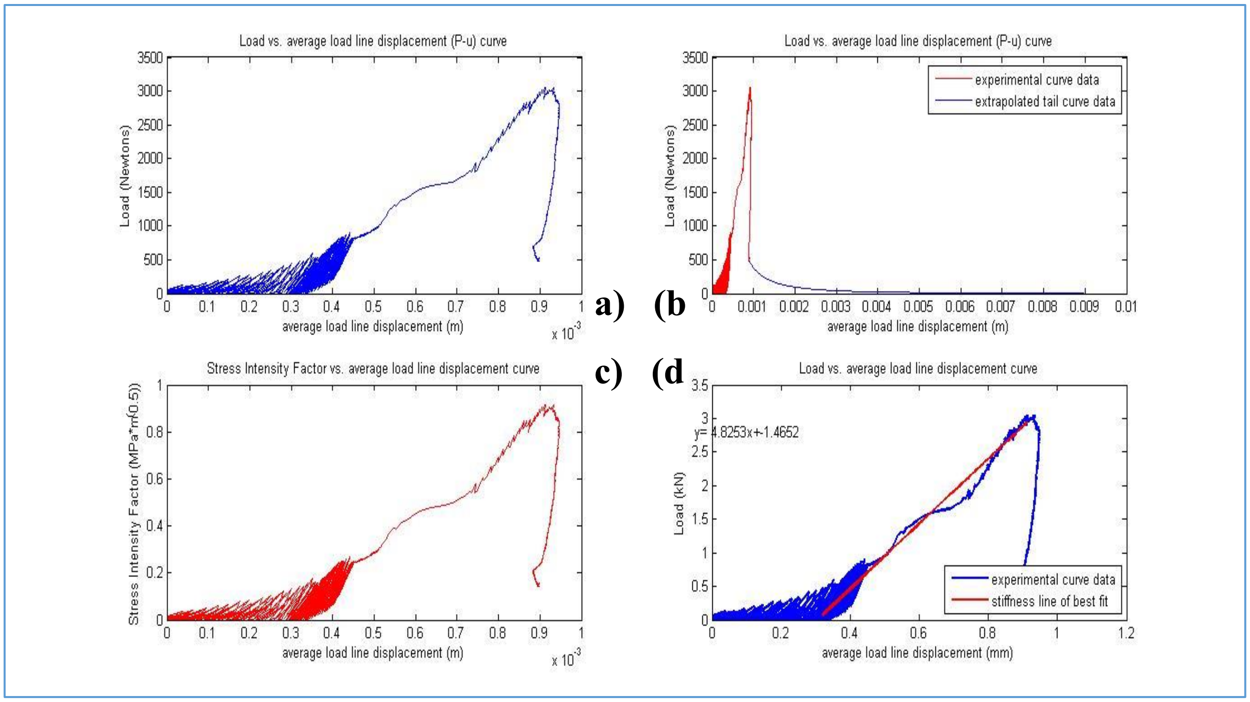

Sample #1) Load-Displacement plot for 35.5% RAP @ -30ºC

a) Load-Displacement, b) tail-end modeling c) stress intensity factor, d) stiffness

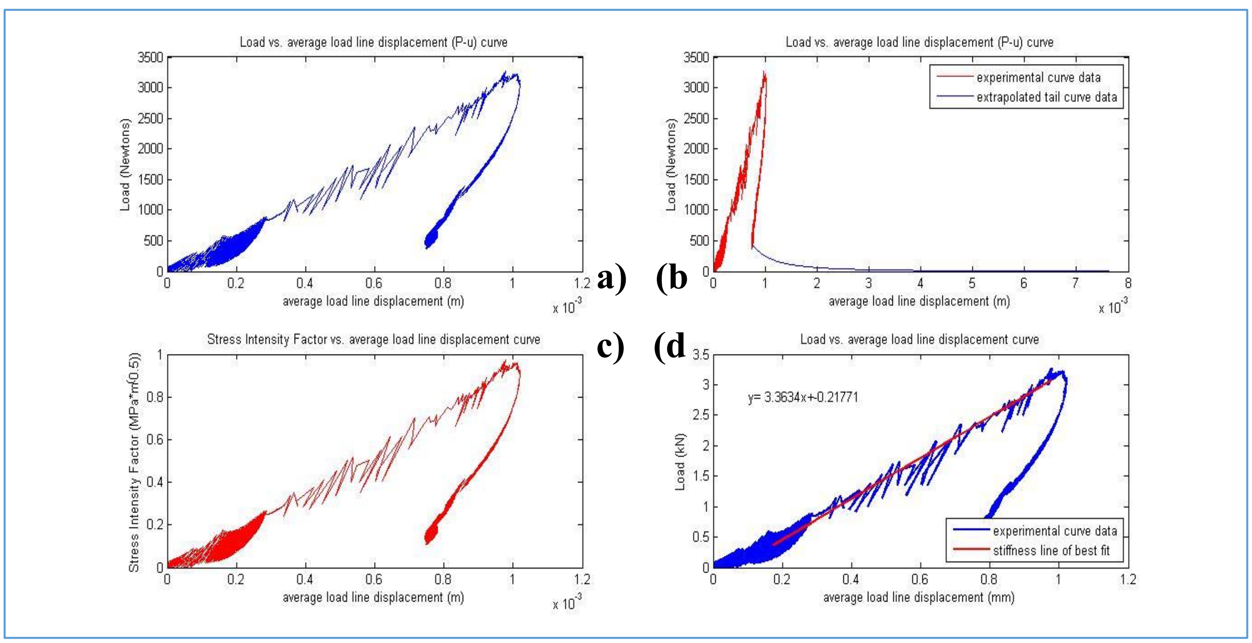

Sample #2) Load-Displacement plot for 35.5% RAP @ -30ºC

a) Load-Displacement, b) tail-end modeling c) stress intensity factor, d) stiffness

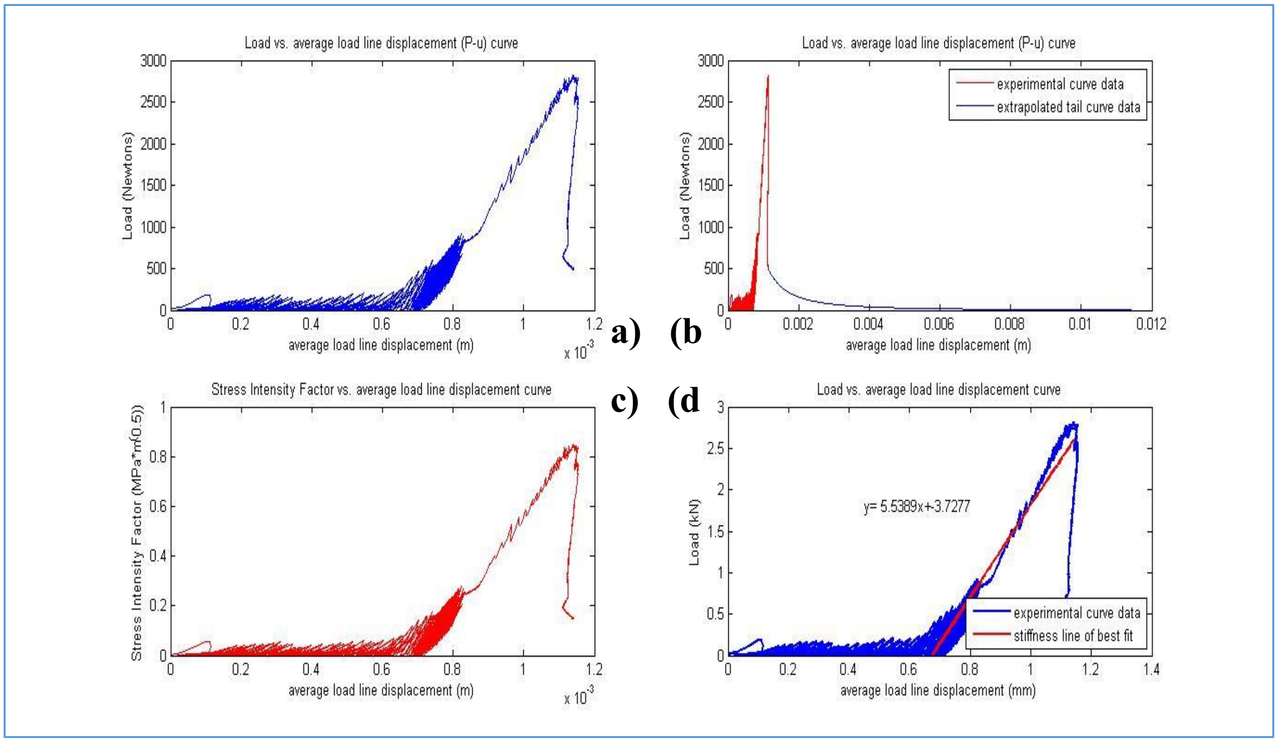

Sample #3) Load-Displacement plot for 35.5% RAP @ -30ºC

a) Load-Displacement, b) tail-end modeling c) stress intensity factor, d) stiffness

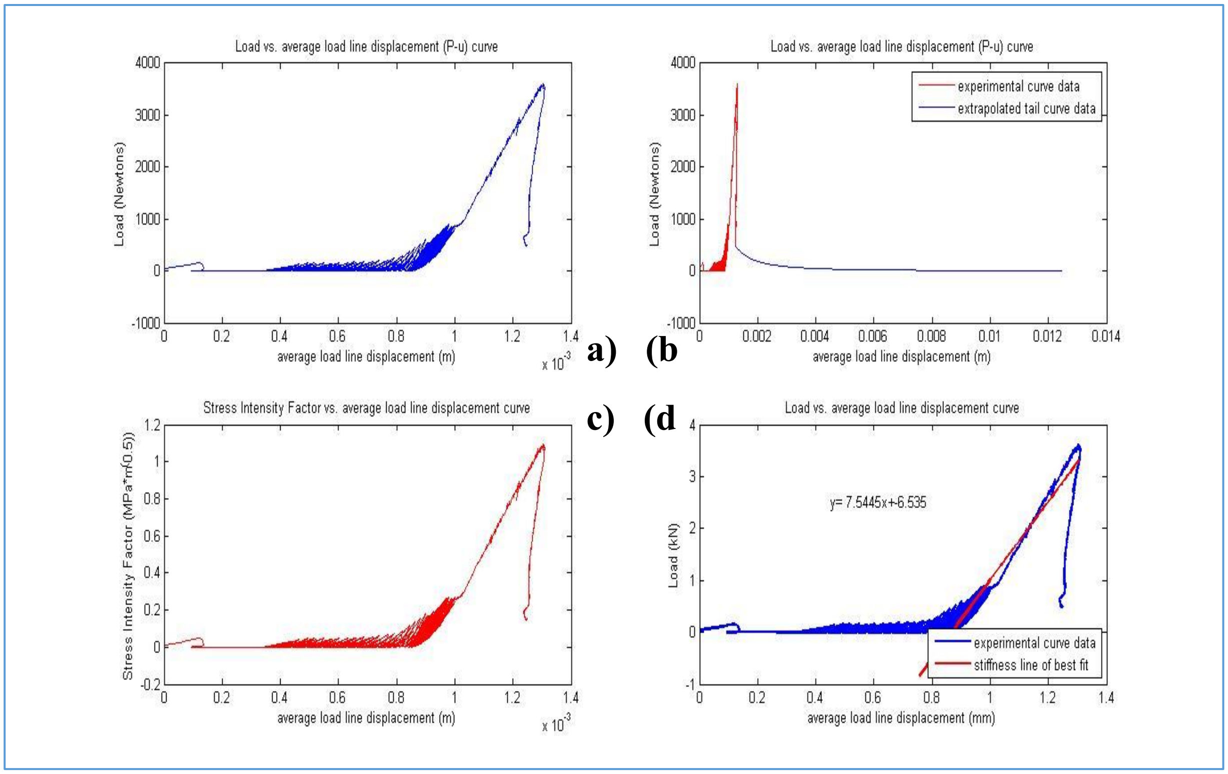

Sample #1) Load-Displacement plot for 35.5% RAP @ -30ºC

a) Load-Displacement, b) tail-end modeling c) stress intensity factor, d) stiffness

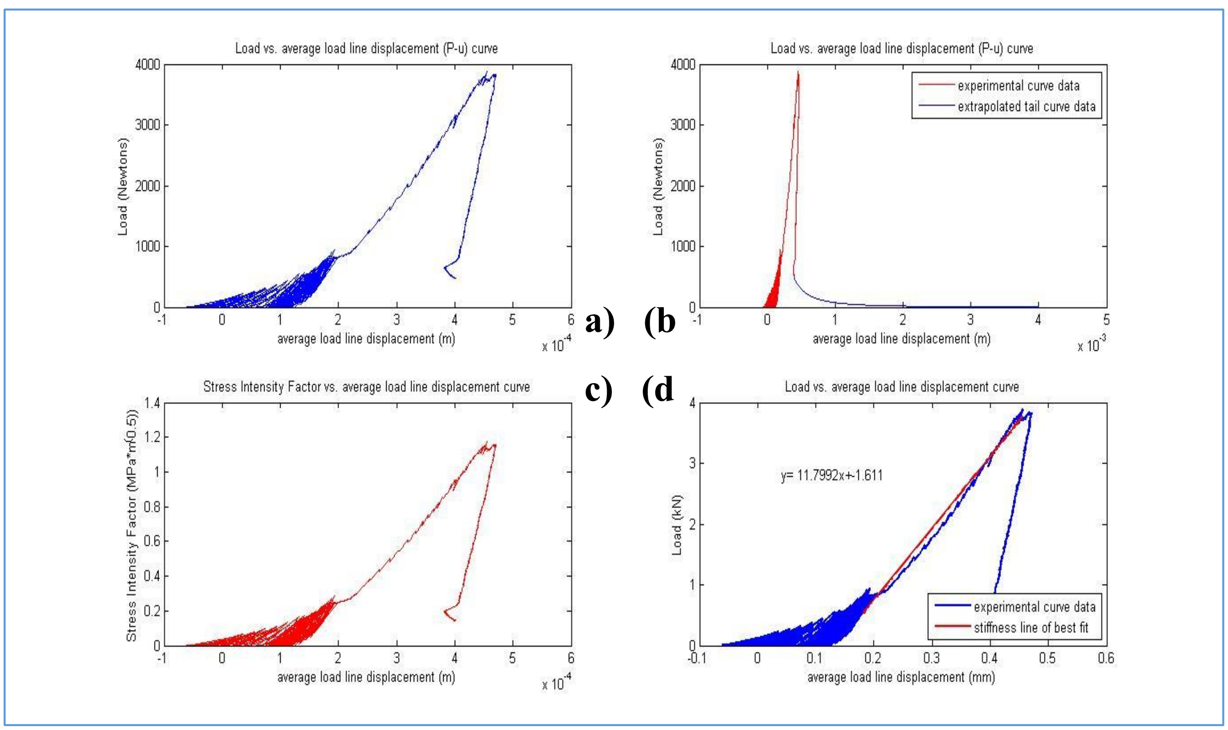

Sample #2) Load-Displacement plot for 35.5% RAP @ -30ºC

a) Load-Displacement, b) tail-end modeling c) stress intensity factor, d) stiffness

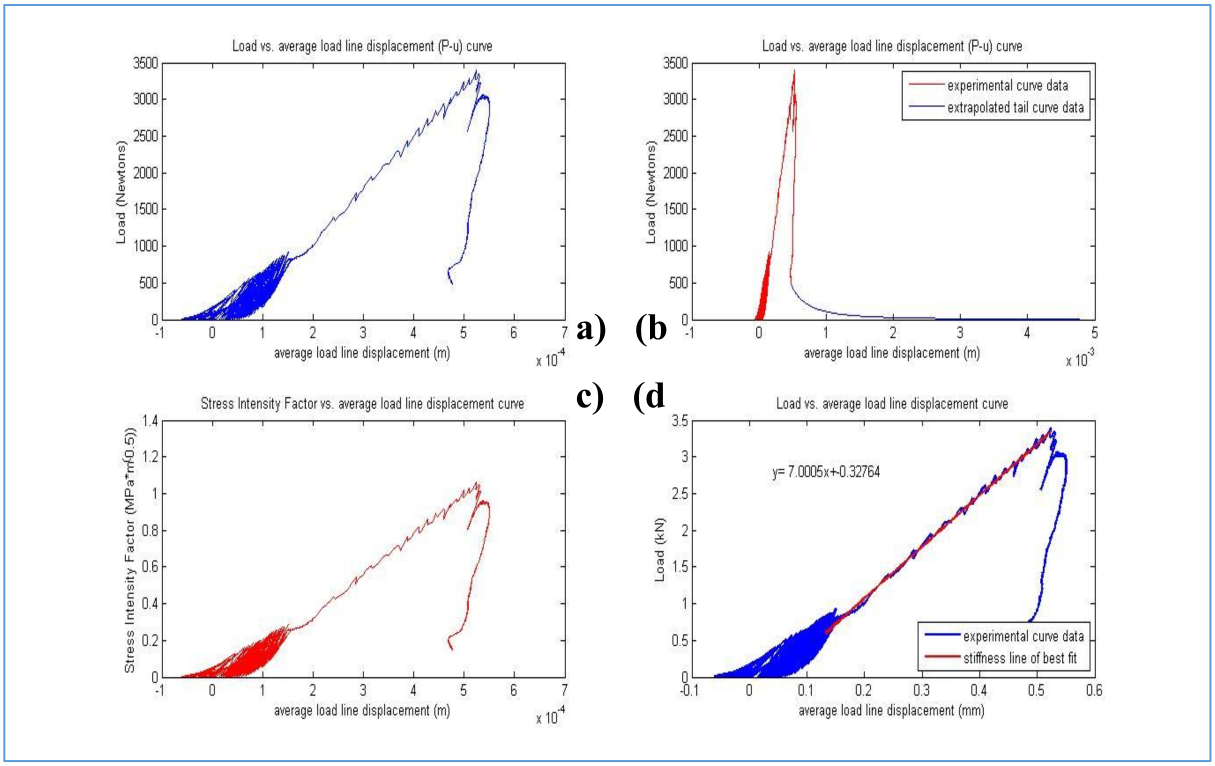

Sample #3) Load-Displacement plot for 35.5% RAP @ -30ºC
a) Load-Displacement, b) tail-end modeling c) stress intensity factor, d) stiffness

Al-Qadi, I. L., M. Elseifi and S. H. Carpenter (2007). "Reclaimed asphalt pavement–a literature review."

Bennert, T., J. S. Daniel and W. Mogawer (2014). Strategies for Incorporating Higher RAP Percentages: Review of Northeast States Implementation Trials. Transportation Research Board 93rd Annual Meeting.

Boriack, P., S. W. Katicha, and G. W. Fintsch (2014). "A Laboratory Study on the Effect of High RAP and High Asphalt Binder Content on the Stiffness, Fatigue Resistance and Rutting Resistance of Asphalt Concrete." 93rd Annual Meeting of the Transportation Research Board.

Buss, A. and R. C. Williams (2013). Investigation of Warm Mix Asphalt for Iowa Roadways– Phase II.

Diefenderfer, S. and H. Nair (2014). Evaluation of High RAP Mixture Production, Construction, and Properties. Transportation Research Board 93rd Annual Meeting.

Huang, B., G. Li, D. Vukosavljevic, X. Shu and B. K. Egan (2005). "Laboratory investigation of mixing hot-mix asphalt with reclaimed asphalt pavement." Transportation Research Record: Journal of the Transportation Research Board 1929(1): 37-45.

Iowa-DOT (2010). "Supplemental Specifications for Recycled Asphalt Pavement (RAP)."

Maupin Jr, G., S. D. Diefenderfer and J. S. Gillespie (2008). Evaluation of Using higher percentages of recycled asphalt pavement in asphalt mixes in Virginia.

McDaniel, R., H. Soleymani and A. Shah (2002). "Use of reclaimed asphalt pavement (RAP) under Superpave specifications: A regional pooled fund project."

McDaniel, R. S., H. Soleymani, R. M. Anderson, P. Turner and R. Peterson (2000). "Recommended use of reclaimed asphalt pavement in the Superpave mix design method." NCHRP Web document 30.

NCAT (2010). "Asphalt Technology News." Vol. 22, No. 1.

Podolsky, J. H., A. Buss, R. C. Williams and E. Cochran (2014). "Comparative performance of bio-derived/chemical additives in warm mix asphalt at low temperature." Materials and Structures: 1-13.

Stephens, J. E., J. Mahoney and C. Dippold (2001). "Determination of the PG Binder Grade to Use in a RAP Mix." Report No. JHR 00-278, Connecticut Department of Transportation.

Tang, S. (2014). "Evaluate The Fracture and Fatigue Resistances of Hot Mix Asphalt Containing High Percentage Reclaimed Asphalt Pavement (RAP) Materials at Low and Intermediate Temperatures." Iowa State Thesis.

Udelhofen, G. (2007). "High RAP Design Works." Asphalt Contractor.

Udelhofen, G. (2010). "Overland Park Successfully Constructs First FRAP Project." Asphalt Contractor.

West, R. C., J. R. Willis and M. O. Marasteanu (2013). Improved mix design, evaluation, and materials management practices for hot mix asphalt with high reclaimed asphalt pavement content, Transportation Research Board.

Wisconsin-DOT (2009). "Section 460 Hot Mix Asphalt Pavement." 2010 Standard Specifications.

Appendix A: SCB Output Graphs

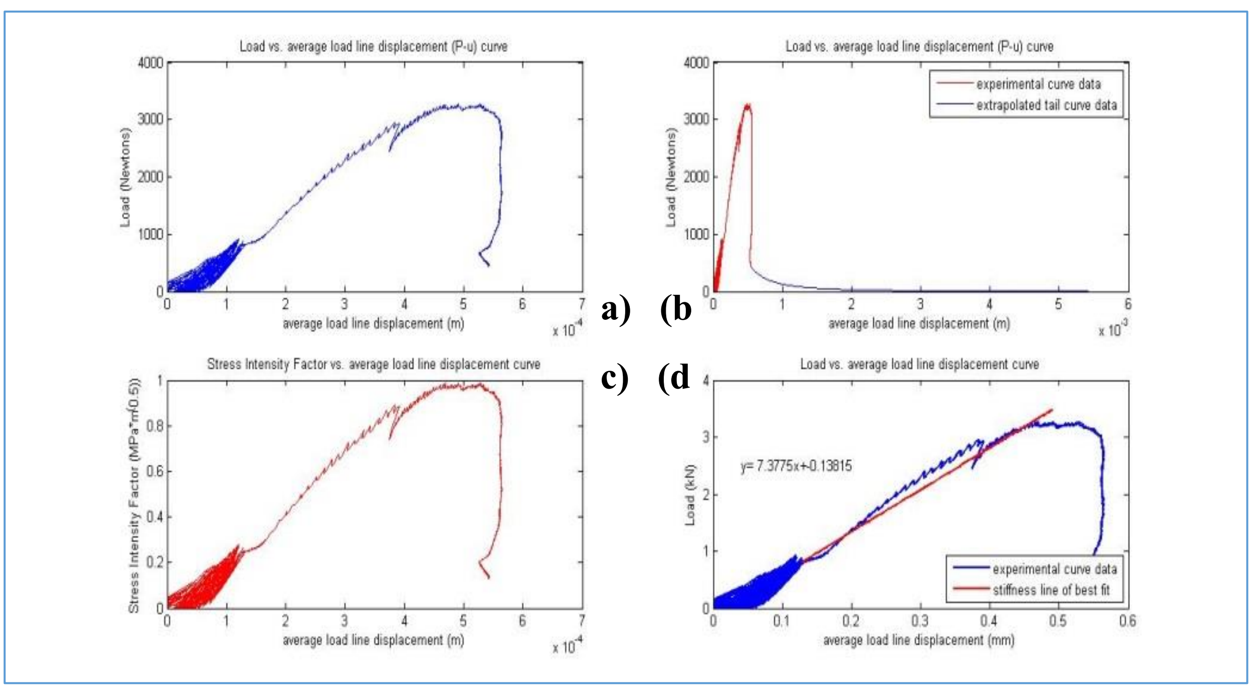

Sample #1) Load-Displacement plot for 30% RAP @ -18 ºC

a) Load-Displacement, b) tail-end modeling c) stress intensity factor, d) stiffness

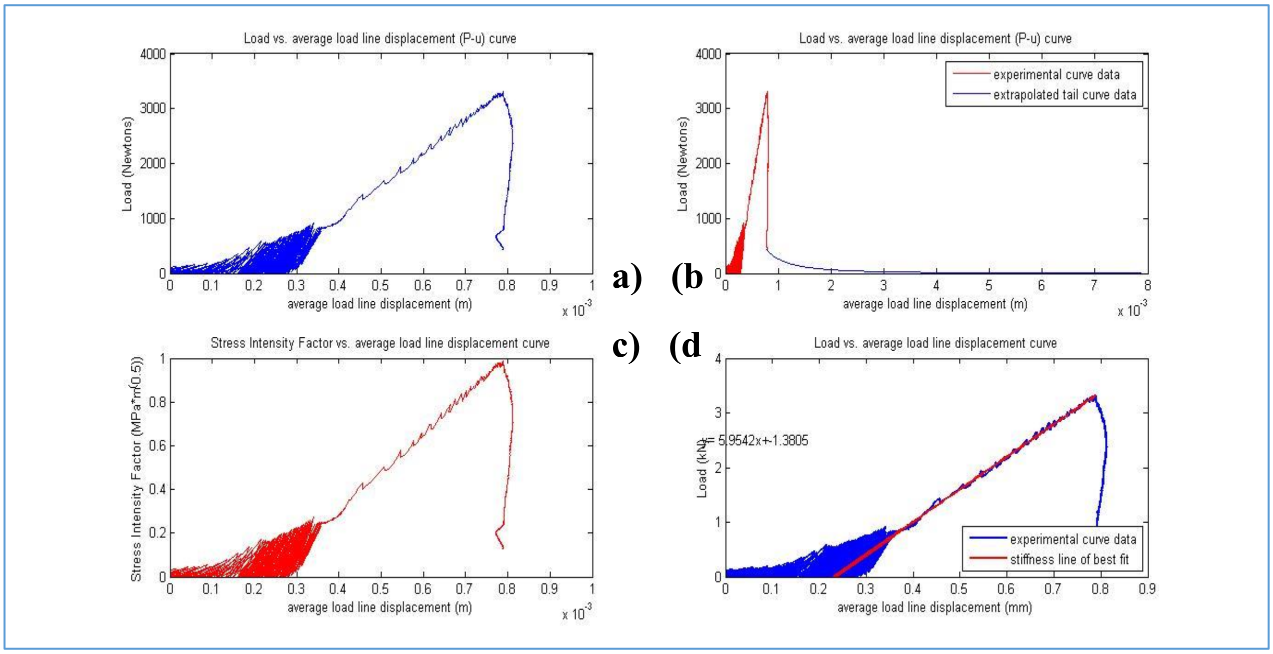

Sample #2) Load-Displacement plot for 30% RAP @ -18 ºC

a) Load-Displacement, b) tail-end modeling c) stress intensity factor, d) stiffness

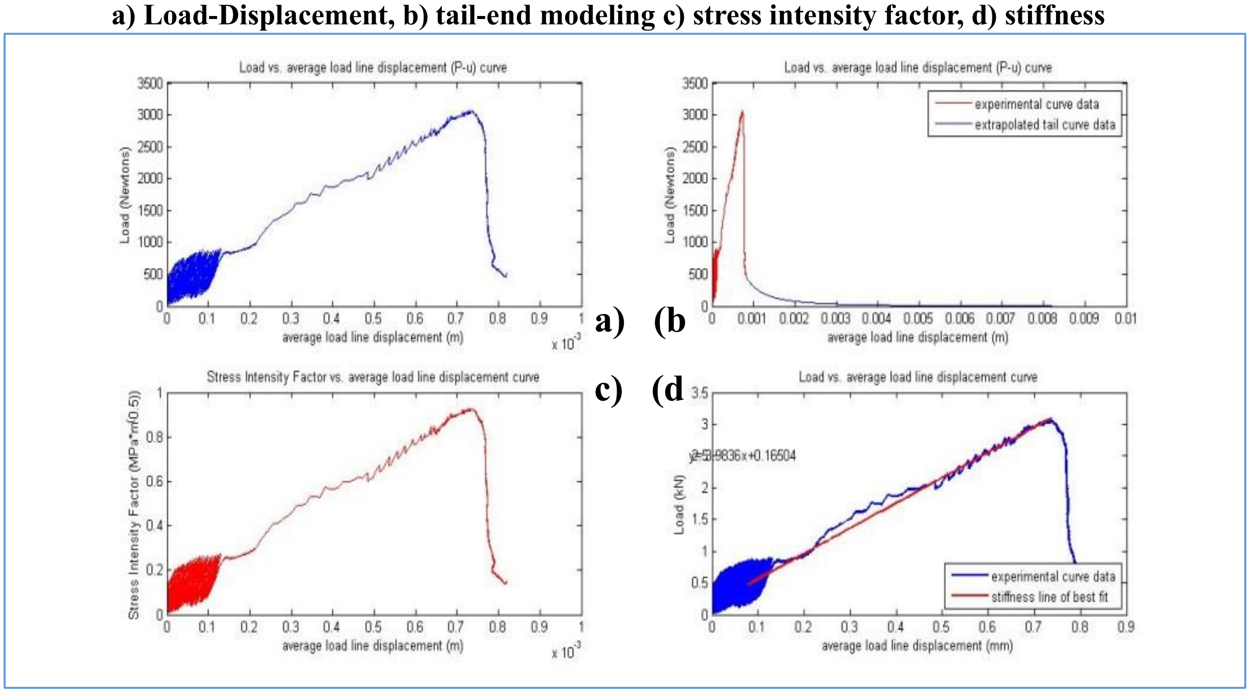

Sample #3) Load-Displacement plot for 30% RAP @ -18 ºC

a) Load-Displacement, b) tail-end modeling c) stress intensity factor, d) stiffness

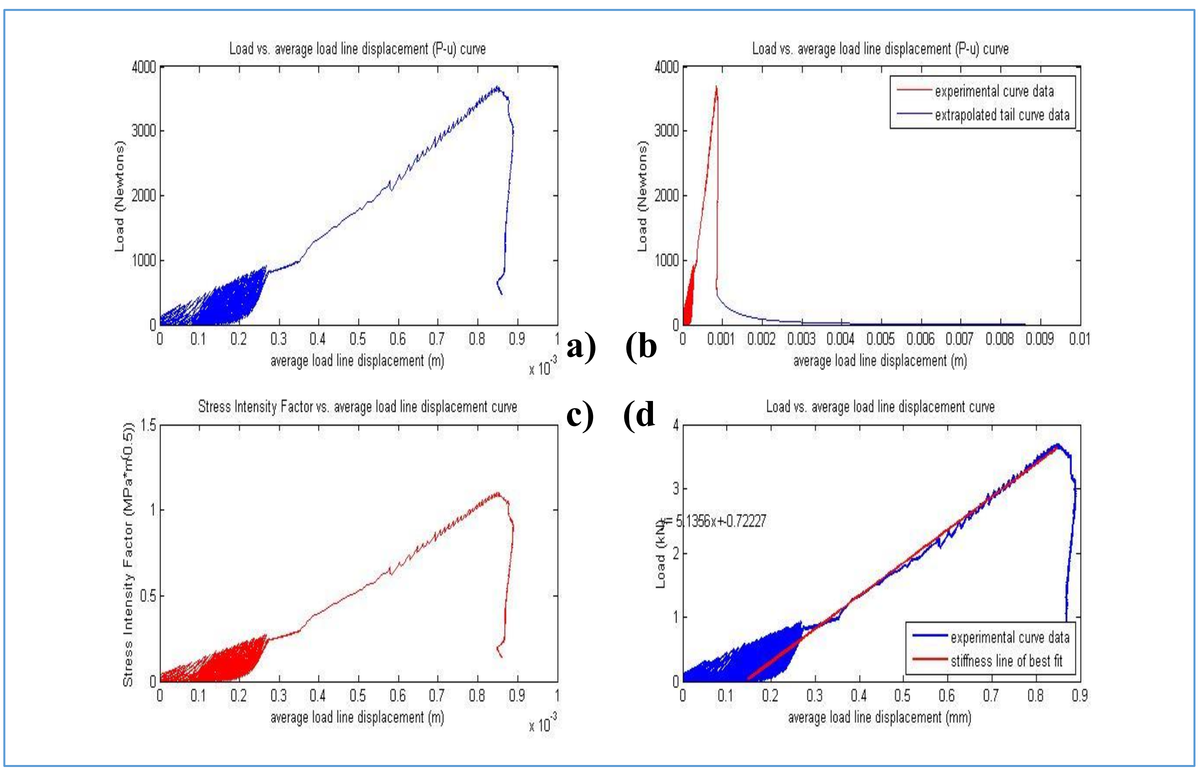

Sample #1) Load-Displacement plot for 35.5% RAP @ -18 ºC

a) Load-Displacement, b) tail-end modeling c) stress intensity factor, d) stiffness

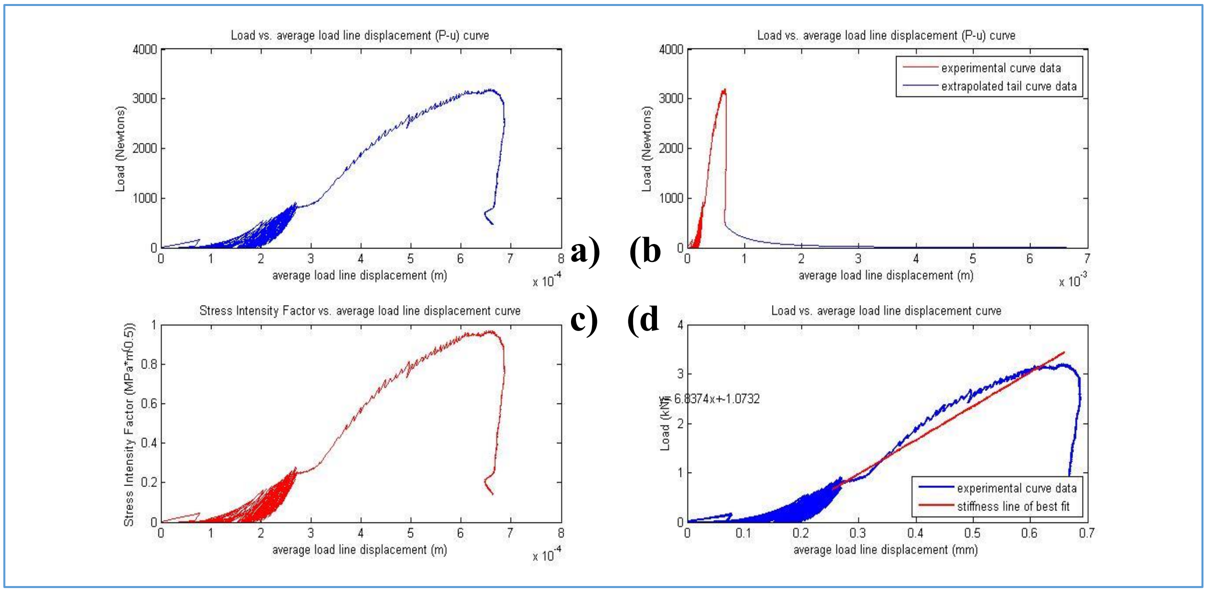

Sample #2) Load-Displacement plot for 35.5% RAP @ -18 ºC

a) Load-Displacement, b) tail-end modeling c) stress intensity factor, d) stiffness

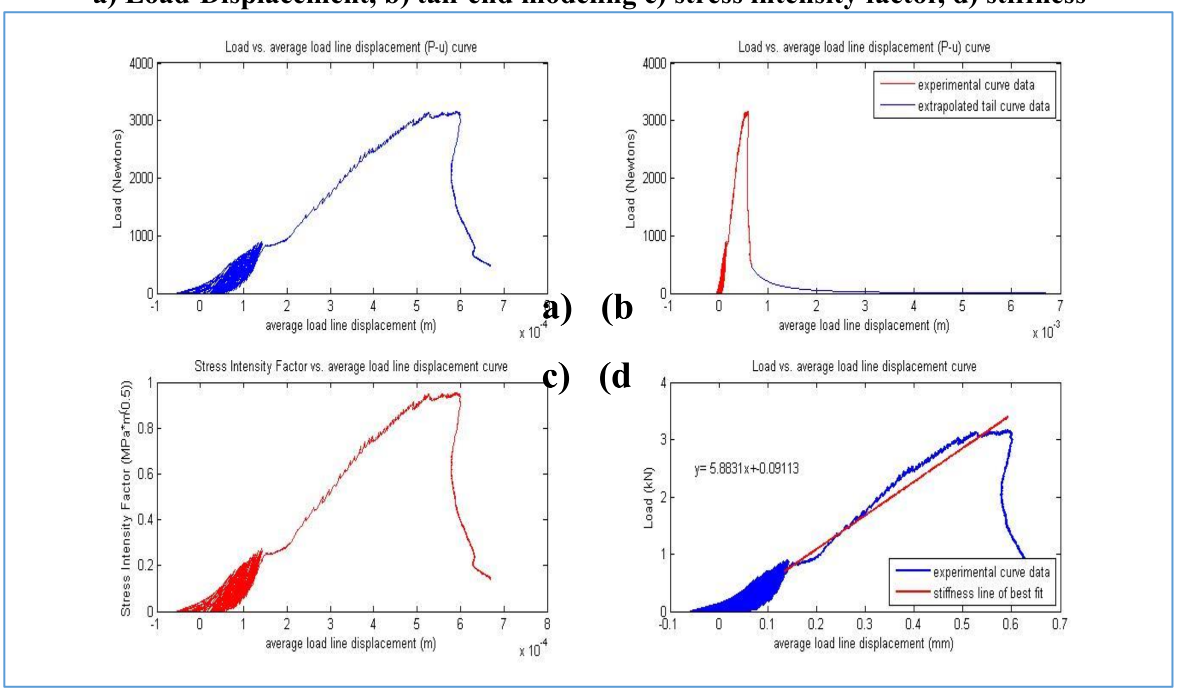

Sample #3) Load-Displacement plot for 35.5% RAP @ -18 ºC

a) Load-Displacement, b) tail-end modeling c) stress intensity factor, d) stiffness

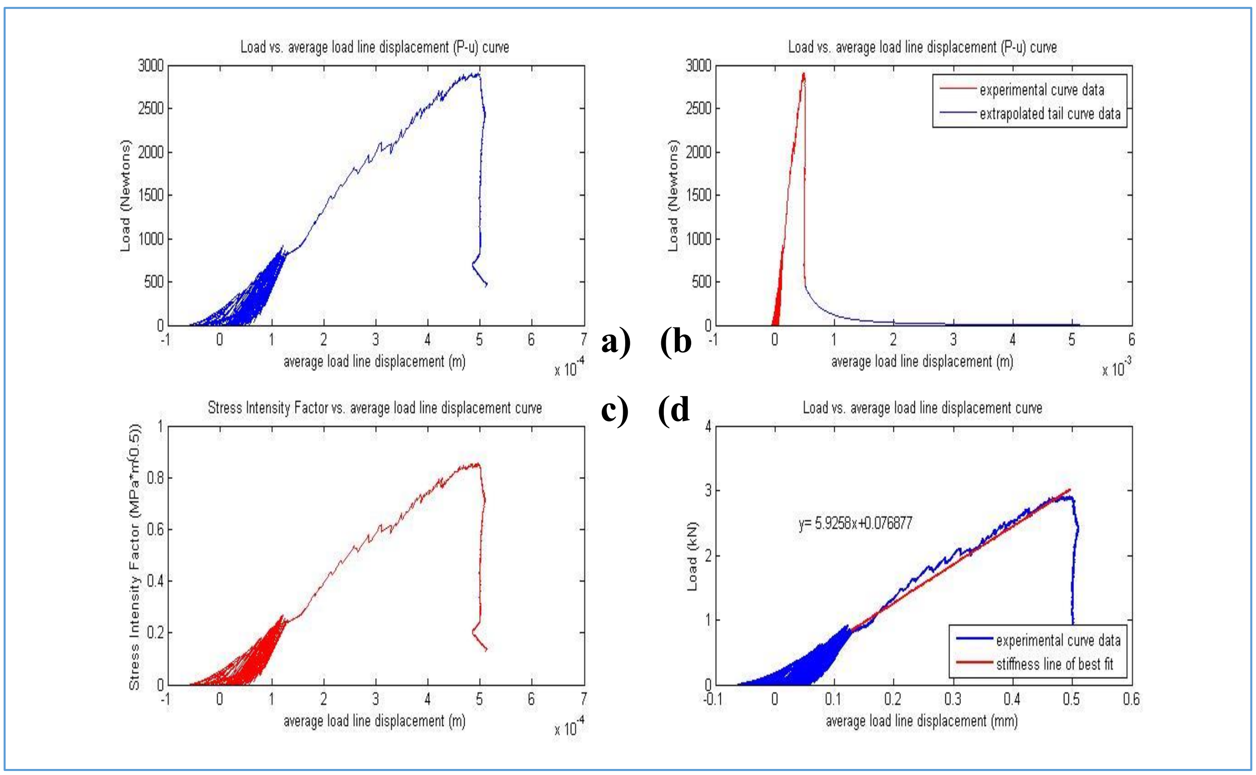

Sample #1) Load-Displacement plot for 39.2% RAP @ -18 ºC

a) Load-Displacement, b) tail-end modeling c) stress intensity factor, d) stiffness

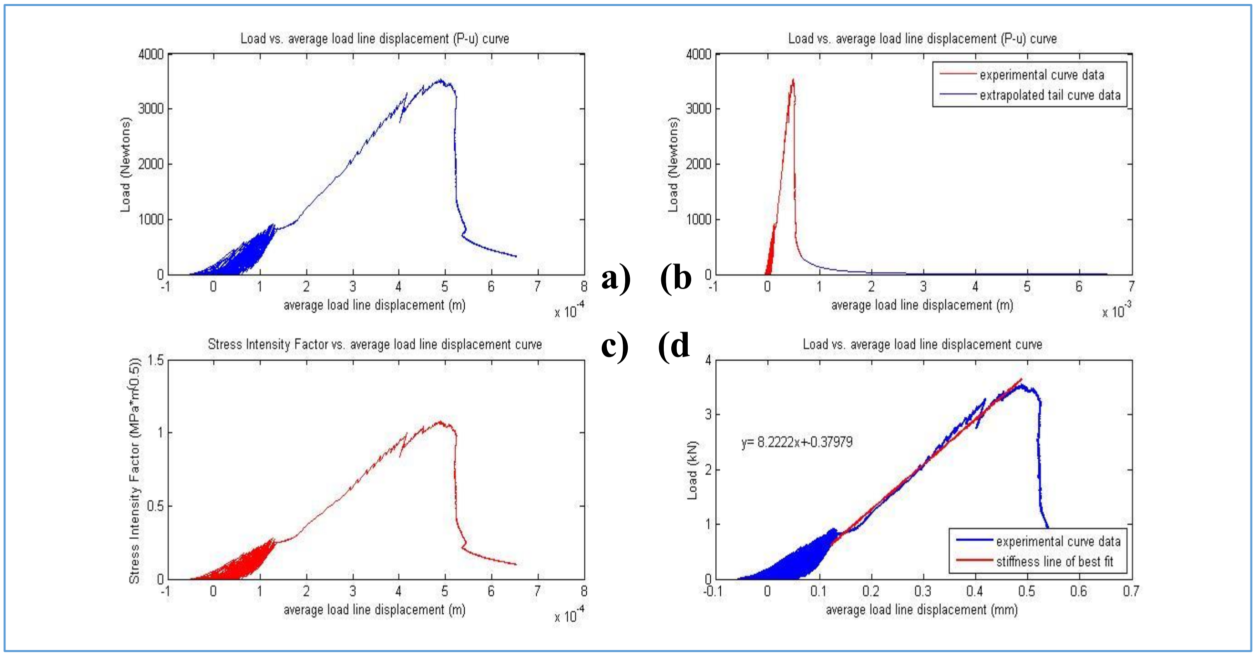

Sample #2) Load-Displacement plot for 39.2% RAP @ -18 ºC

a) Load-Displacement, b) tail-end modeling c) stress intensity factor, d) stiffness

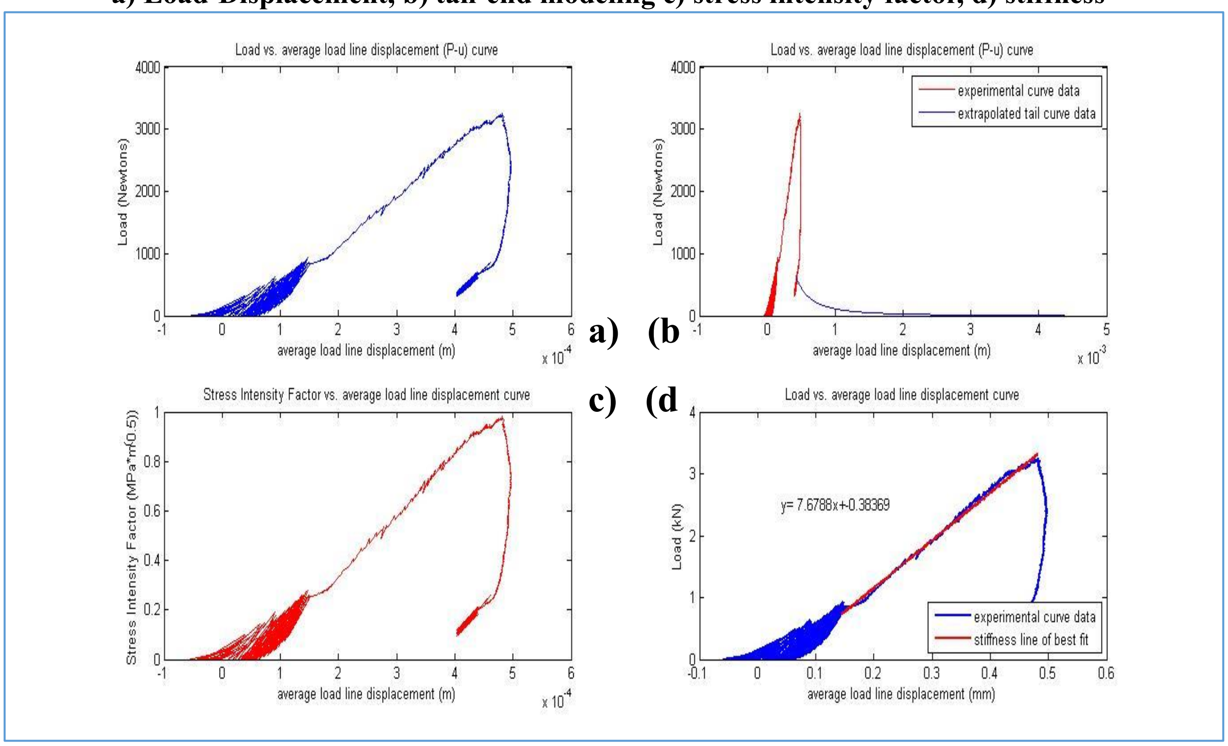

Sample #3) Load-Displacement plot for 39.2% RAP @ -18 ºC

a) Load-Displacement, b) tail-end modeling c) stress intensity factor, d) stiffness

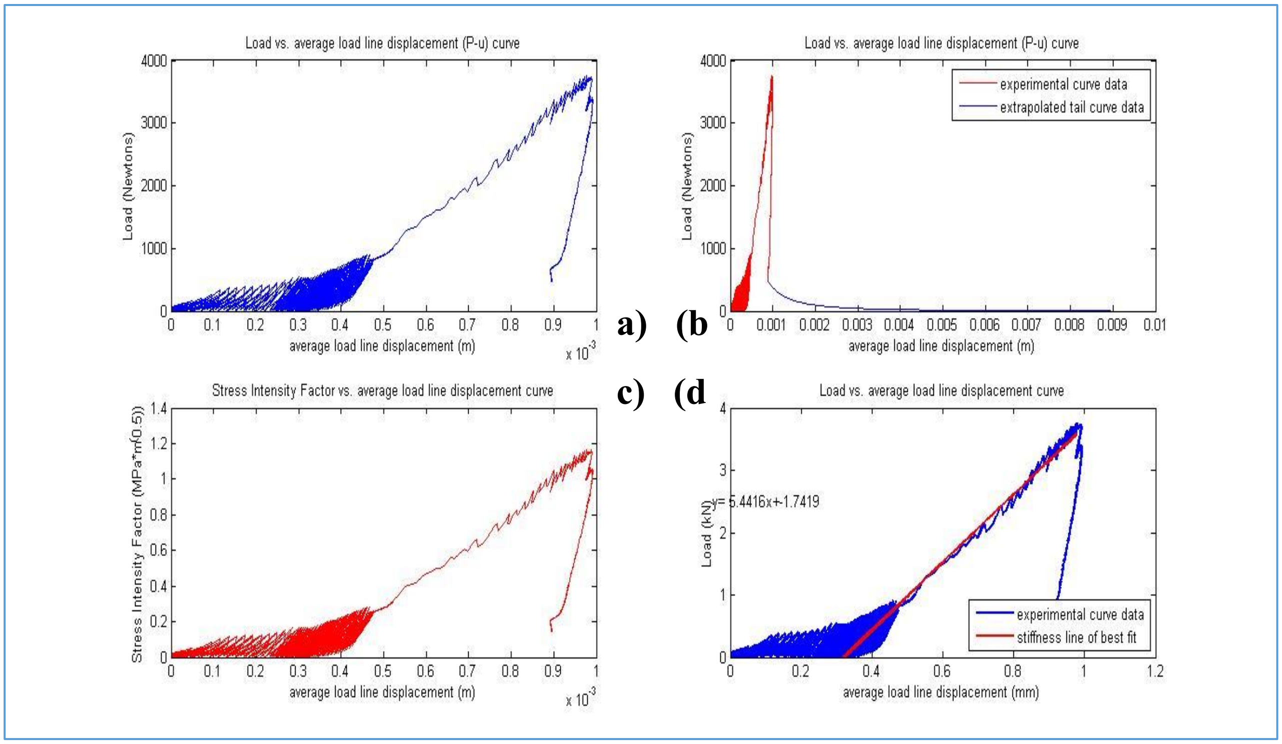

Sample #1) Load-Displacement plot for 30% RAP @ -30ºC

a) Load-Displacement, b) tail-end modeling c) stress intensity factor, d) stiffness

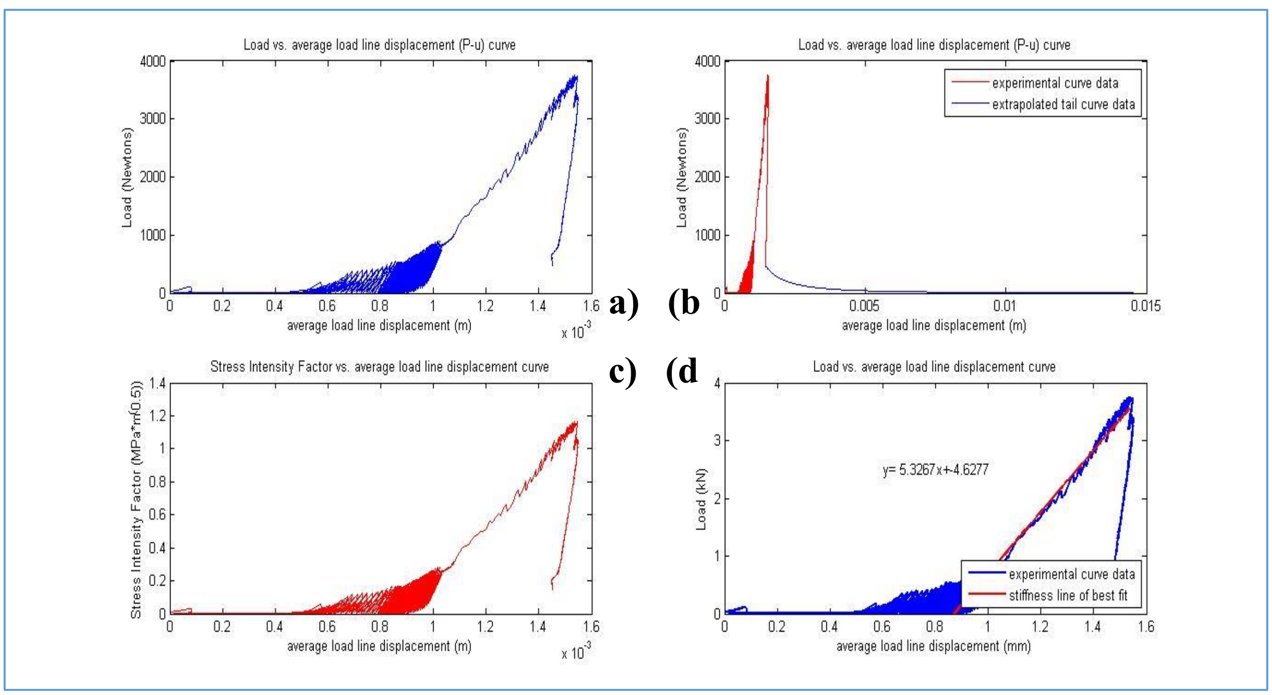

Sample #2) Load-Displacement plot for 30% RAP @ -30ºC

a) Load-Displacement, b) tail-end modeling c) stress intensity factor, d) stiffness

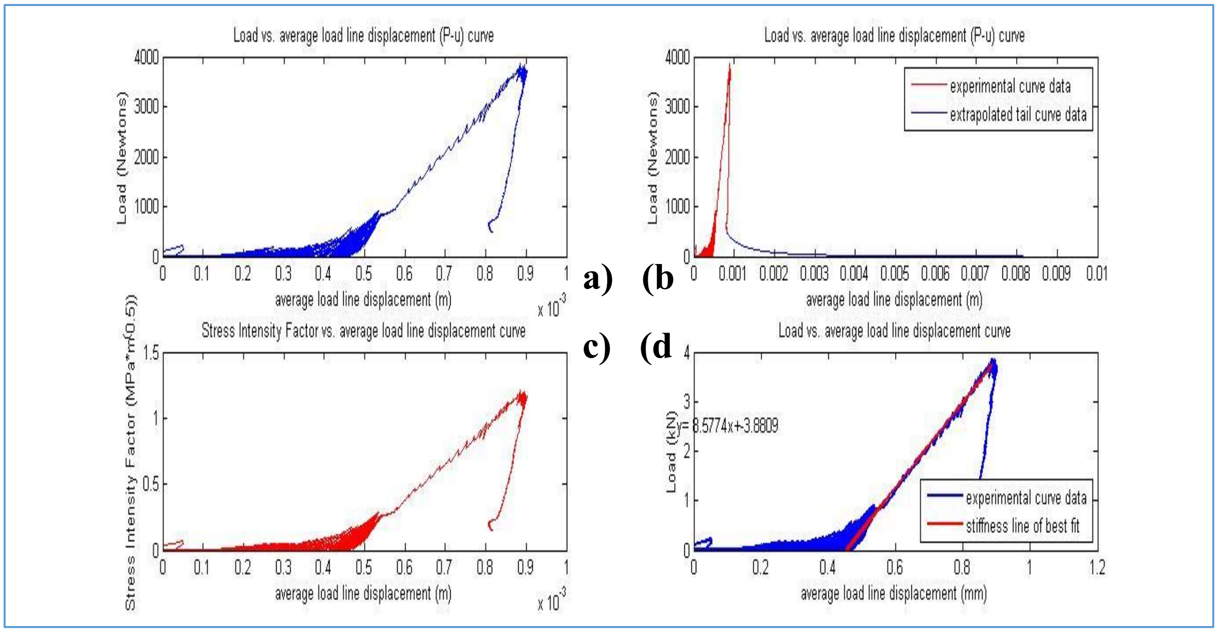

Sample #3) Load-Displacement plot for 30% RAP @ -30ºC

a) Load-Displacement, b) tail-end modeling c) stress intensity factor, d) stiffness

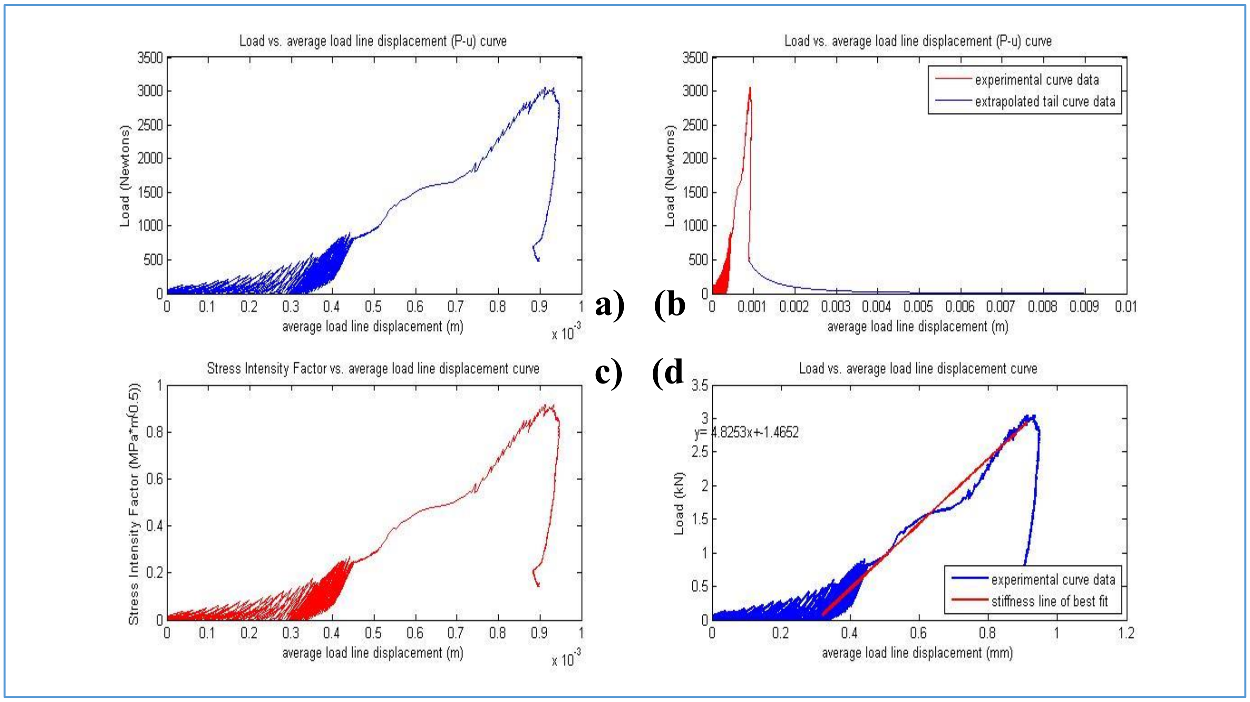

Sample #1) Load-Displacement plot for 35.5% RAP @ -30ºC

a) Load-Displacement, b) tail-end modeling c) stress intensity factor, d) stiffness

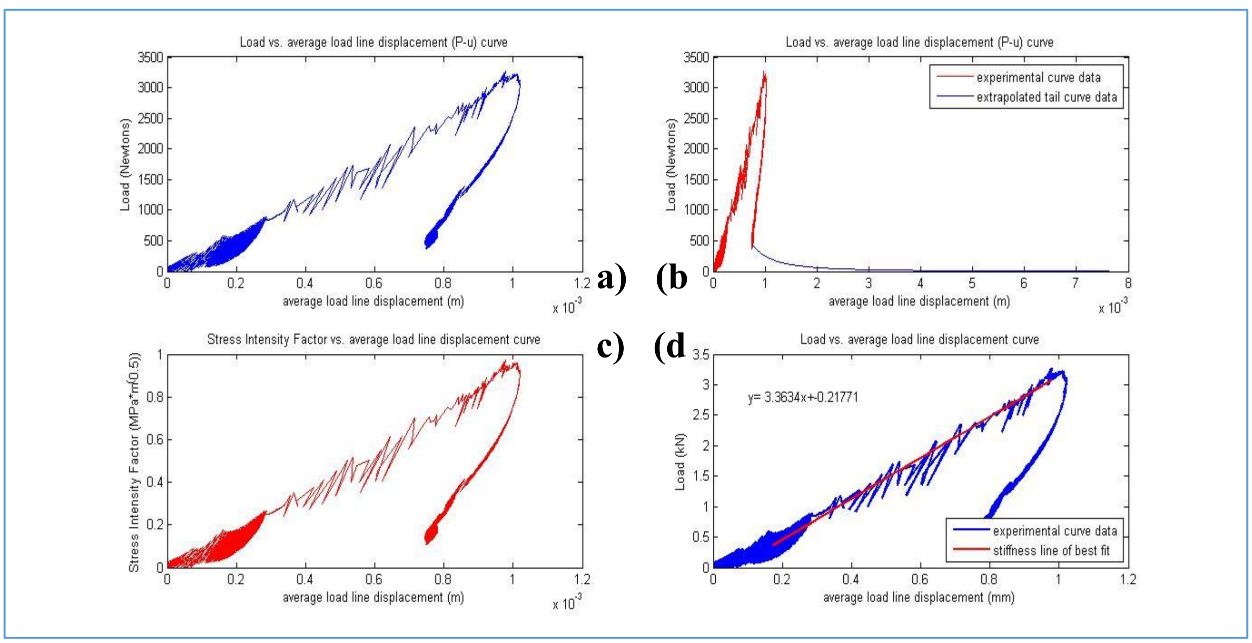

Sample #2) Load-Displacement plot for 35.5% RAP @ -30ºC

a) Load-Displacement, b) tail-end modeling c) stress intensity factor, d) stiffness

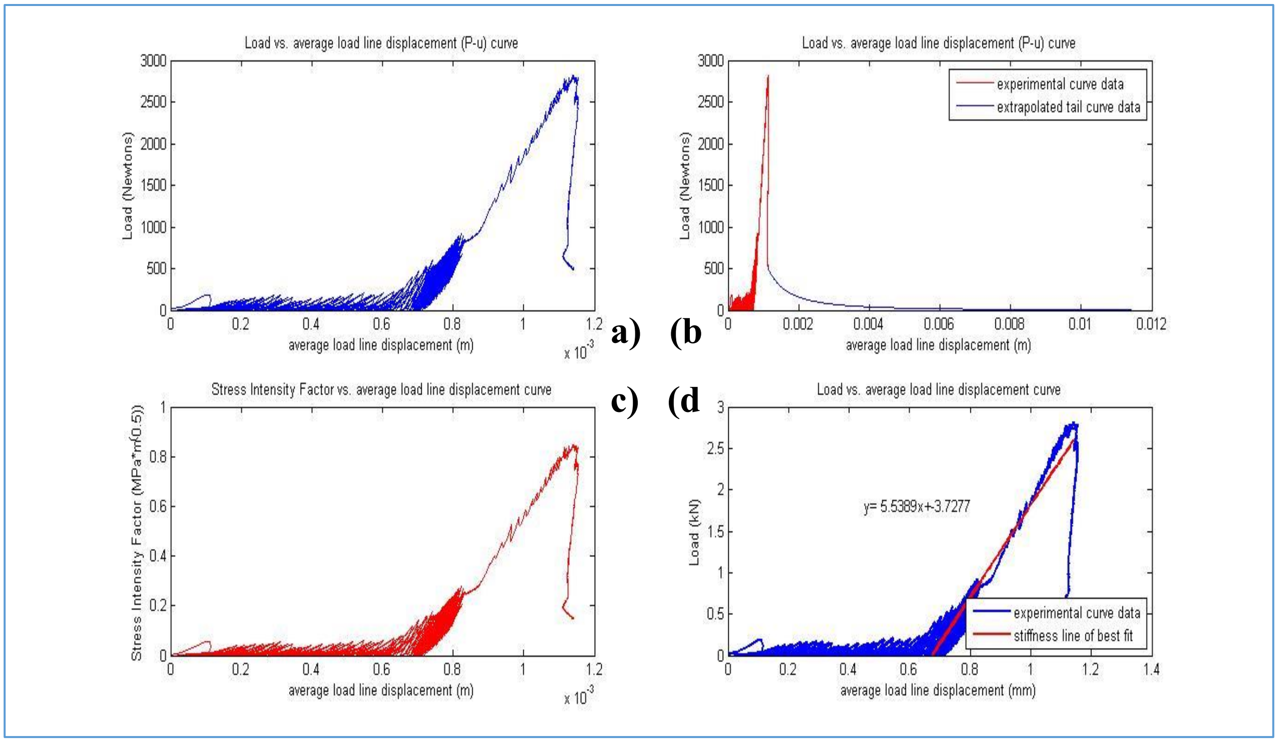

Sample #3) Load-Displacement plot for 35.5% RAP @ -30ºC

a) Load-Displacement, b) tail-end modeling c) stress intensity factor, d) stiffness

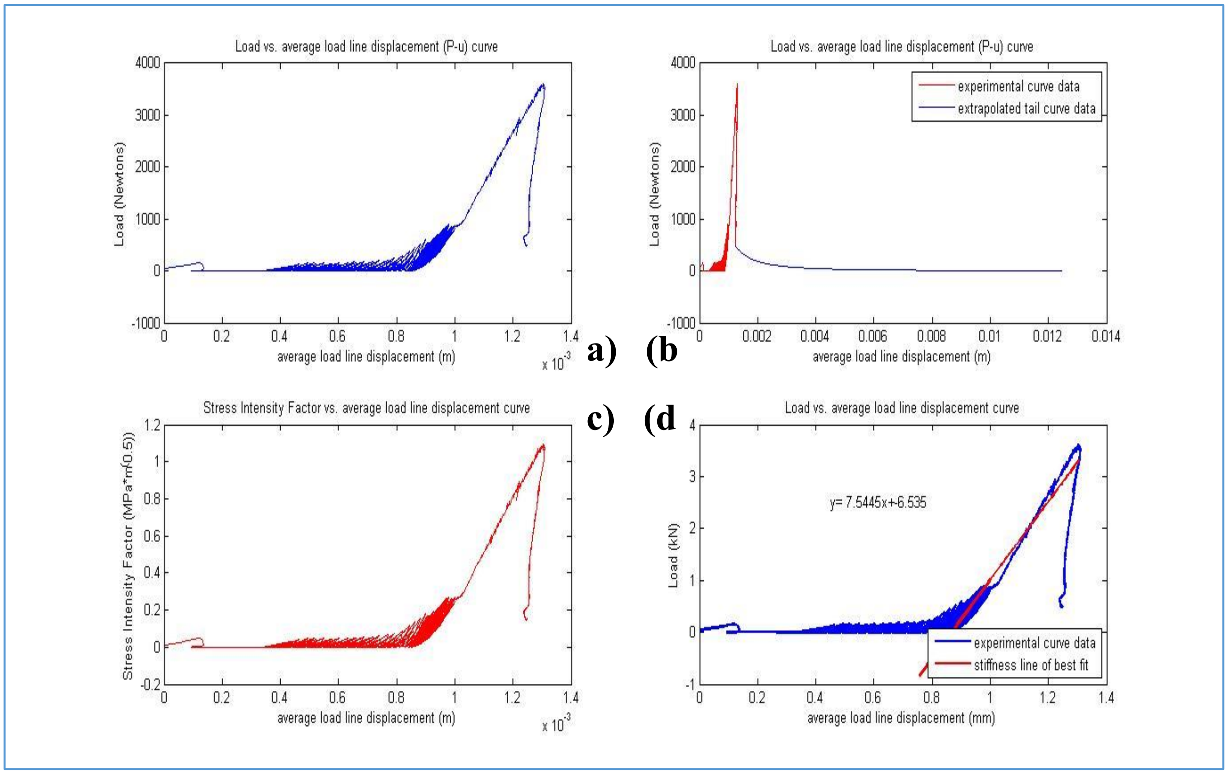

Sample #1) Load-Displacement plot for 35.5% RAP @ -30ºC
a) Load-Displacement, b) tail-end modeling c) stress intensity factor, d) stiffness

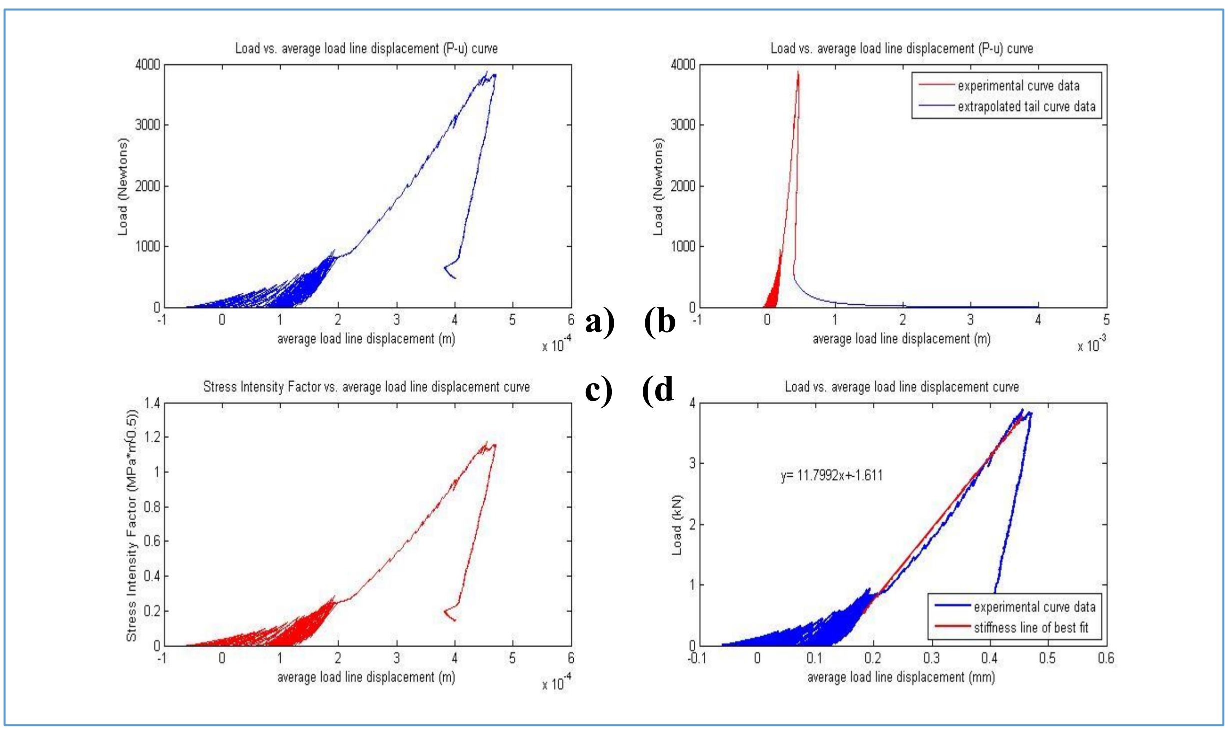

Sample #2) Load-Displacement plot for 35.5% RAP @ -30ºC
a) Load-Displacement, b) tail-end modeling c) stress intensity factor, d) stiffness

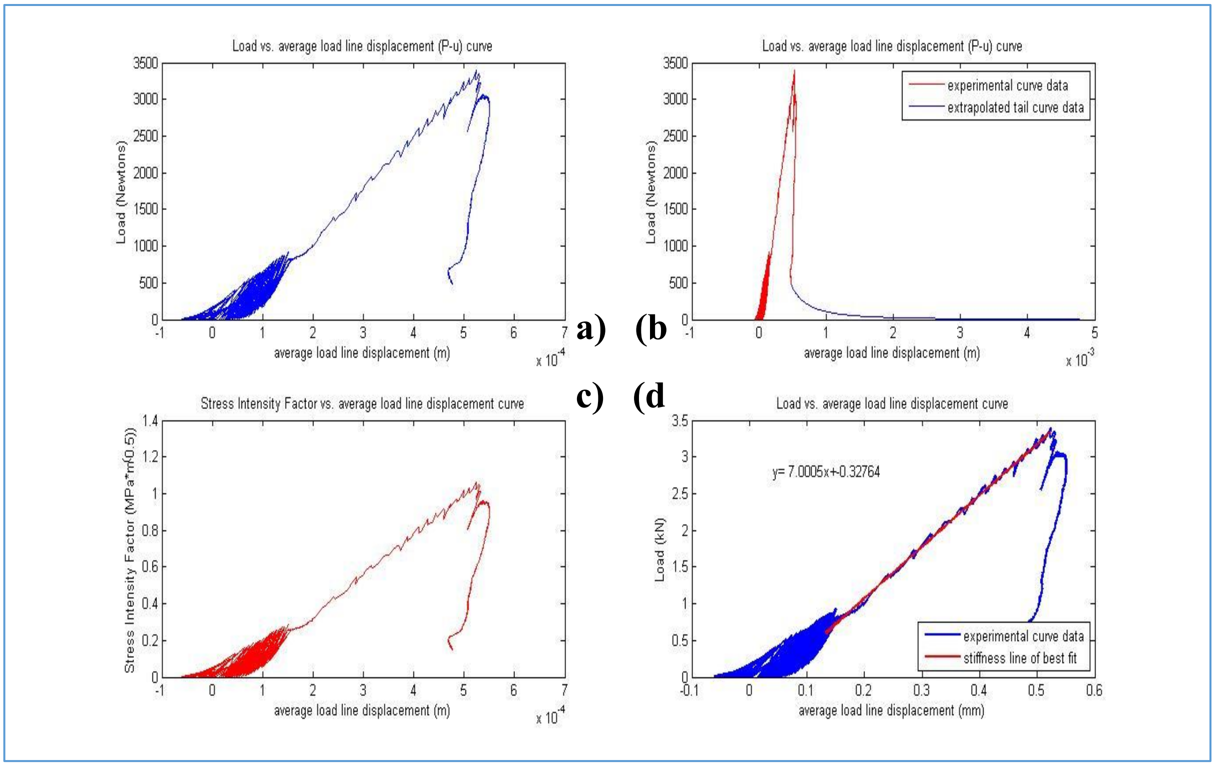

Sample #3) Load-Displacement plot for 35.5% RAP @ -30ºC

a) Load-Displacement, b) tail-end modeling c) stress intensity factor, d) stiffness